UNIVERSIDADE FEDERAL DO RIO GRANDE DO SUL
INSTITUTO DE CIÊNCIAS BÁSICAS DA SAÚDE
PROGRAMA DE PÓS-GRADUAÇÃO EM CIÊNCIAS BIOLÓGICAS: BIOQUÍMICA

Detecção da atividade da purino nucleosídeo fosforilase (EC 2. 4. 2. 1) em líquido cérebro espinhal de rato e determinação de estrutura tridimensional e parâmetros cinéticos da enzima humana recombinante com 7-metil-6-tio-guanosina

Rafael Guimarães da Silva

Dissertação apresentada ao Programa de Pós-Graduação em Ciências Biológicas: Bioquímica, da Universidade Federal do Rio Grande do Sul, como pré-requisito para obtenção do grau de Mestre em Bioquímica

Orientadores: Prof. Dr. Diógenes Santiago Santos
Prof. Dr. Luiz Augusto Basso

Porto Alegre, 2005

Dedico este trabalho à Claudete Guimarães da Silva e à Hebraima Guimarães, por seu incentivo e apoio incondicionais.

Este trabalho foi realizado, em sua maior parte, no Laboratório de Microbiologia Molecular e Funcional do Departamento de Biologia Molecular e Biotecnologia da Universidade Federal do Rio Grande do Sul, e no Centro de Pesquisas em Biologia Molecular e Funcional da Pontifícia Universidade Católica do Rio Grande do Sul, sob orientação dos Professores Diógenes Santiago Santos e Luiz Augusto Basso. Parte do trabalho foi desenvolvida no Laboratório de Sistemas Biomoleculares do Departamento de Física da Universidade Estadual Paulista, sob responsabilidade do Professor Walter Filgueira de Azevedo Jr.

Agradecimentos

Aos meus orientadores, **Diógenes Santiago Santos** e **Luiz Augusto Basso**, pela oportunidade inigualável de trabalhar sob sua orientação, bem como pela amizade, generosidade e confiança demonstradas ao longo desses anos.

Aos Professores **Walter Filgueira de Azevedo Jr.**, **Mário Sérgio Palma**, **João Batista Calixto** e **Osmar Norberto de Souza**, por me receberem em seus laboratórios e por seus ensinamentos.

Aos Professores **Diogo Onofre de Souza**, **Susana Wofchuk** e **Luis Walmor Portela**, pela colaboração e incentivo.

Aos amigos **Isabel Osorio**, **Rodrigo Ducati**, **Jaim Oliveira**, **Isabel Werlang**, **Clarissa Czekster**, **Diego Viali**, **Christopher Schneider**, **Luiz Pedro Sório** e **Maria de Lurdes Magalhães**, com os quais estou sempre aprendendo.

Às colegas **Clotilde Amorin Pinto** e **Renilda Trapp**, por manterem o laboratório funcionando.

Aos colegas **Alessandro Silva**, **Juliano Murad**, **Patrícia Webber**, **Fernanda Ely**, **Caroline Rizzi**, **Ana Luiza Vivan**, **Raquel Schwanke**, **Gaby Renard**, **Jocelei Chies**, **Igor Vasconcelos** e **Bruna Selbach**, pelo convívio e parceria.

À secretaria do PPG-Bioquímica, principalmente à **Cléia Bueno**, pela competência e ajuda com a burocracia.

Ao **Programa de Pós-Graduação em Bioquímica**, pela oportunidade de desenvolver o mestrado.

Ao **CNPq/Ministério da Ciência e Tecnologia**, pela bolsa de mestrado.

Índice

Lista de Figuras

1. Introdução

3. Artigo 1: Purine nucleoside phosphorylase activity in rat cerebrospinal fluid

4. Artigo 2: Crystal structure and kinetics of human purine nucleoside phosphorylase in complex with 7-methyl-6-thio-guanosine

Lista de Tabelas

Abreviaturas

PNP	Purino nucleosídeo fosforilase
P_i	Fosfato inorgânico
Glu	Glutamato
Phe	Fenilalanina
Asn	Asparagina
Arg	Arginina
Ser	Serina
His	Histidina
C	Carbono
pM	Picomolar
Å	Angstron
MESG	7-metil-6-tio-guanosina
K_M	Constante de Michaelis
V	Velocidade Máxima
ε	Coeficiente de absortividade molar
M	Molar
cm	centímetro
K_{cat}	Constante catalítica
μM	Micromolar
pH	potencial hidrogeniônico
s	segundo

Resumo

A enzima purino nucleosídeo fosforilase catalisa a clivagem reversível da ligação *N*-ribosídica de nucleosídeos purínicos, gerando ribose 1-fosfato e a base púrica correspondente. Esta é uma etapa importante na via de salvamento de purinas, controlando o fluxo de compostos a ser excretados, na forma de ácido úrico, e revertendo-o para a formação de nucleotídeos, de acordo com a necessidade celular. Essa atividade enzimática é ubíqua, entretanto apresenta importância fundamental em linfócitos-T, visto que a ausência dessa enzima em humanos, característica de uma desordem genética, acarreta morte a tais células, embora todos os outros tipos celulares permaneçam normais. Esse fato suscitou um grande interesse nessa enzima, pois drogas que a inibam poderiam ser empregadas como imunossupressores, visando à intervenção clínica em casos de doenças auto-imunes, leucemias e linfomas de células-T e rejeição de órgãos transplantados. Com o intuito de desenvolver inibidores da enzima, seu mecanismo catalítico tem sido amplamente estudado. Recentemente, foi demonstrado que nucleosídeos purínicos são capazes de proteger células cerebrais expostas a danos quimicamente induzidos, indicando que a purino nucleosídeo fosforilase possa exercer também algum papel nesse processo. Com o objetivo de adquirir maior conhecimento a respeito da interação da enzima humana com seus ligantes, estudos cinéticos e estruturais da mesma foram realizados, utilizando 7-metil-6-tio-guanosina, um nucleosídeo sintético, como substrato, possibilitando a interpretação dos parâmetros cinéticos em nível atômico. Numa abordagem para investigar o possível papel da purino nucleosídeo fosforilase na proteção de células nervosas, a atividade dessa enzima foi medida em líquido cérebro espinhal de rato, demonstrando, pela primeira vez, sua presença em meio extracelular, seguido de uma caracterização cinética aparente da enzima, utilizando o substrato supracitado. Os resultados com a enzima humana podem auxiliar no desenvolvimento de novas drogas contra desordens do sistema imunológico, enquanto o trabalho com líquido cérebro espinhal de rato é um passo inicial almejando a elucidação da função da via de catabolismo de purinas em células cerebrais.

Abstract

The enzyme purine nucleoside phosphorylase catalyzes the reversible cleavage of *N*-ribosidic bonds of purine nucleosides, generating ribose 1-phosphate and the corresponding purine base. That is an important step of purine salvage pathway, controlling the flow of compounds to be excreted, in uric acid form, and reverting it to the nucleotide formation, according to the cellular demand. This enzymatic activity is ubiquitous, nevertheless it is vital in T lymphocytes, since the lack of that enzyme in humans, due to a genetic disorder, leads to impairment of such cells, though keeping normal other tissues. This fact has attracted a large interest in purine nucleoside phosphorylase, since drugs capable of inhibiting this enzyme might be employed as immune-modulators, aiming at developing clinical procedures in cases of autoimmune diseases, leukemia and lymphomas, and organ transplantation rejection. With the intent of developing purine nucleoside phosphorylase inhibitors, its catalytic mechanism has been widely studied. Recently, purine nucleotides were demonstrated to protect brain cells exposed to chemically-induced injuries, and a role for purine nucleoside phosphorylase in this process was suggested. With the goal of acquiring a better knowledge about the interaction between the human enzyme and its ligand molecules, kinetic and structural studies were performed, utilizing 7-methyl-6-thio-guanosine, a synthetic nucleoside, as substrate, allowing the interpretation of kinetic parameters at atomic level. As an approach to investigate the role of this enzyme in neuron protection, its activity was measured in rat cerebrospinal fluid, which showed, for the first time, its presence in extra-cellular medium, followed by an apparent kinetic characterization of the enzyme with the substrate cited above. Results with the human enzyme can aid the development of new drugs against immunological disorders, whereas those concerning rat cerebrospinal fluid are and initial step towards elucidating the function of purine catabolism pathway in brain cells.

1. Introdução

As desordens relacionadas ao sistema imunológico, como neoplasias e doenças auto-imunes, afetam milhões de pessoas no mundo inteiro, contribuindo para a diminuição da qualidade de vida das mesmas, levando-as muitas vezes à morte. Em países como os Estados Unidos, uma média anual de 12 casos de leucemia são diagnosticados para cada 100.000 habitantes, e acredita-se que essa seja uma tendência mundial (Ries *et al.*, 2004).

Quanto às doenças auto-imunes, como lupus, psoríase, artrite reumatóide e síndrome de Crohn, caracterizadas pela reatividade de células imunológicas contra tecidos do próprio organismo, estima-se que haja cerca de 1 bilhão de pacientes em todo o planeta. Como ainda não se têm uma cura definitiva para tais enfermidades, tratamentos paliativos tentam, com pouco sucesso, diminuir seus sintomas (Heimer, 1999).

A busca de novos fármacos capazes de intervir de maneira mais eficaz contra as doenças supracitadas faz-se necessária, bem como a identificação de alvos específicos sobre os quais esses fármacos agiriam. Durante a década de 1970, foram relatados casos de crianças com a síndrome da imunodeficiência severa congênita, nas quais constatava-se morte seletiva de linfócitos-T, enquanto as células-B e os outros tecidos permaneciam normais. Como causa para tal síndrome, propunha-se a ausência de atividade da enzima purino nucleosídeo fosforilase (PNP) (E. C. 2. 4. 2. 1), devida a mutações nos *loci* que a codificam (Giblett *et al.*, 1975; Stoop *et al.*, 1977). Assim, essa enzima passou a ser considerada um alvo potencial para o desenvolvimento de drogas, almejando ao tratamento de desordens do sistema imunológico em que as células-T desempenhem algum papel importante (Stoeckler, 1984). Isso suscitou um grande interesse por essa enzima, resultando em inúmeros trabalhos abordando diversos aspectos.

1. 1 A enzima purino nucleosídeo fosforilase

A enzima purino nucleosídeo fosforilase (purina-ortofosfato; ribosil transferase) faz parte da via de salvamento de purinas, a qual é responsável pela conversão de nucleotídeos purínicos em ácido úrico e vice-versa (Parks e Agarwal, 1972). A PNP catalisa a clivagem reversível de nucleosídeos e desoxinucleosídeos purínicos, exceto adenosina e desoxiadenosina, na presença de fosfato inorgânico (P_i), gerando ribose 1-fosfato ou desoxirribose 1-fosfato e a base púrica correspondente (Kalckar, 1947), invertendo a configuração de β-nucleosídeo para α-ribose 1-fosfato (Stoeckler, Cambor e Parks, 1980). Embora o equilíbrio da reação seja deslocado para a síntese de nucleosídeos, em células intactas a fosforólise é favorecida pelo acoplamento com a enzima xantina oxidase, a última enzima da via (Parks e Agarwal, 1972). A reação catalisada pela PNP é apresentada na Figura 1.

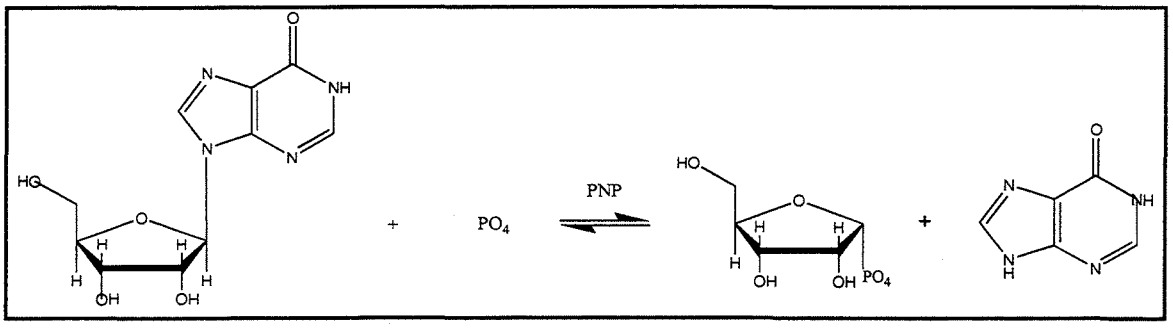

Figura 1: Reação catalisada pela enzima purino nucleosídeo fosforilase. O grupo fosfato é adicionado à posição C1' da inosina, e os produtos hipoxantina e α-ribose 1-fosfato são liberados da enzima.

Estudos de especificidade de substrato revelam que a PNP exibe grande preferência por purinas contendo grupamento ceto na posição 6, em vez de grupamento amino (Zimmerman *et al.*, 1971). Quanto ao açúcar, a enzima apresenta forte especificidade por ribose, em comparação com os estereoisômeros arabinose, xilose e lixose (Stoeckler *et al.*, 1980).

Com o intuito de se desvendar seu mecanismo cinético, as PNPs humanas e bovinas têm sido isoladas a partir de várias fontes, como eritrócitos, baço, fígado e cérebro (Kim, Cha e Parks, 1968a; Bzowska *et al.*, 1995; Silva *et al.*, 2003; Lewis e Glantz, 1976). Embora vários trabalhos indiquem um mecanismo seqüencial, a ordem de adição dos substratos à enzima ainda não é um consenso. No final da década de 1960, estudos cinéticos com PNP humana propunham um mecanismo obrigatoriamente ordenado em que o nucleosídeo ligava-se à enzima antes do P_i (Kim, Cha e Parks, 1968b). Dados mais recentes apontam exatamente o oposto: inosina e guanosina não se ligam à PNP na ausência de P_i (Porter, 1992). Contradizendo esse último resultado, foi demonstrado que a enzima é capaz de hidrolisar inosina na ausência de P_i (Kline e Schramm, 1992). Estruturas tridimensionais da PNP foram obtidas tanto em complexo com sulfato (ocupando o sítio de P_i), como associada à inosina (Ealick *et al.*, 1990; de Azevedo *et al.*, 2003a; Mao *et al.*, 1998). Logo, uma ordem aleatória de adição dos substratos à enzima ainda não é descartada.

No que tange seu mecanismo catalítico, os resultados apresentam um grau maior de concordância. A construção de formas mutantes da enzima, por mutações pontuais em códons que codificam aminoácidos do sítio ativo, permitiu a avaliação de quais resíduos são realmente importantes para ligação dos substratos e ou catálise. No sítio de ligação do nucleosídeo, os aminoácidos considerados essenciais para ligação do substrato são Glu201 e Phe200, enquanto Asn243 parece estar envolvida na catálise. Os resíduos de Arg84, Ser33 e His86, no sítio de ligação a P_i, desempenham algum papel na catálise (Erion *et al.*, 1997). Análises de efeitos isotópicos cinéticos foram empregadas como tentativa de elucidar o mecanismo catalítico da reação, tanto para hidrólise quanto para arsenólise de inosina. Concluiu-se que a reação ocorre pela protonação da base nitrogenada através da Asn243, formação de um oxocarbênio e concomitante rompimento da ligação ribosídica, o que precede a ligação do grupamento arsenato (em vez de P_i) (Kline e Schramm, 1992; Kline e Schramm, 1993; Kline e Schramm, 1995). A partir de tais informações, foi sugerido um modelo para o estado de transição da reação catalisada pela PNP (Figura 2). A partir desse, foi desenhado e sintetizado um composto análogo ao estado de transição, o imucilina-H (1S-1-9-deaza-hipoxantina-1-4-didesoxi-1-imino-D-ribitol), o qual inibe as PNPs humana e bovina com constantes de inibição (K_i) de 74 pM e 23 pM, respectivamente (Miles *et al.*, 1998). Esse inibidor é capaz de impedir o crescimento de linfócitos-T ativados (Kicska

et al., 2001) e encontra-se em fase II de testes clínicos (Bantia *et al.*, 2003). Apesar disso, continuam os esforços para se entender melhor o sítio ativo da enzima e sua interação com moléculas de substrato, produto e inibidores, tentando-se desenvolver drogas ainda mais potentes do que a imucilina-H.

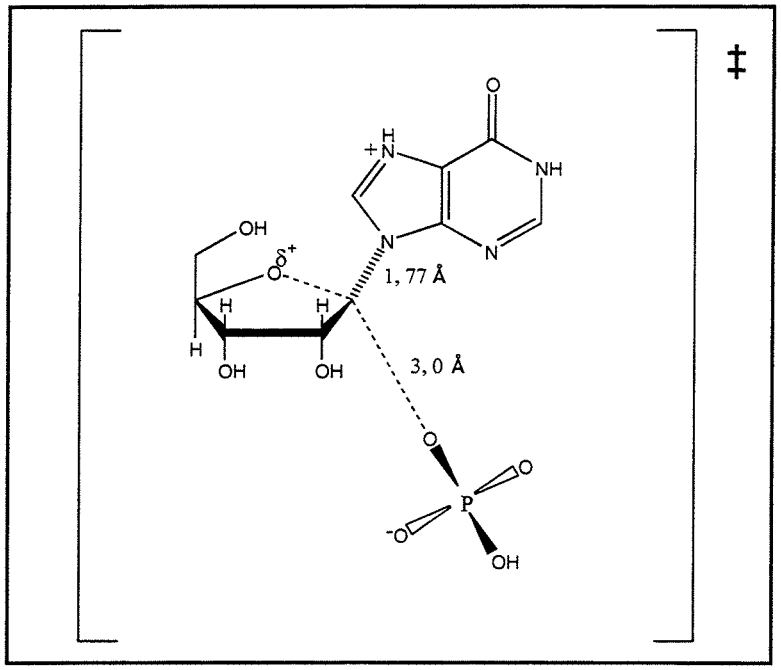

Figura 2: Modelo proposto por Kline e Schramm para o estado de transição da reação catalisada pela PNP bovina, o qual apresenta um caráter de oxocarbênio. A base nitrogenada fica positivamente carregada, enquanto a ligação *N*-ribosídica estende-se para 1, 77 Å de comprimento. O grupamento fosfato aproxima-se até a distância de 3, 0 Å, para formação da com o C1' da ribose.

1. 2 Estudos estruturais

Desde o início da década de 1990, a cristalografia por difração de raios – X tem sido utilizada para determinar a estrutura da PNP humana, e a estrutura obtida serviu como modelo para o desenho racional de drogas (Ealick *et al.*, 1990; Ealick *et al.*, 1991). Isso estimulou a determinação de estruturas tridimensionais de PNPs de outras fontes, tanto bacterianas como de mamíferos, gerando grande número de informações sobre as características tridimensionais da enzima e interações da mesma com seus ligantes (Tebbe *et al.*, 1999; Shi *et al.*, 2001; de Azevedo *et al.*, 2003b; dos Santos *et al.*, 2003).

A PNP apresenta-se como um trímero tanto em solução como na forma cristalina (de Azevedo *et al.*, 2003c), e cada monômero é constituído por folhas-β circundadas de α-hélices, com o sítio ativo situado na extremidade C-terminal de uma folha-β central (Figura 3), característico das PNPs triméricas da família de nucleosídeo fosforilases NP-I, segundo uma classificação estrutural (Pugmire e Ealick, 2002). A natureza das interações entre o sítio ativo e os substratos tem sido elucidada a partir da co-cristalização da enzima na presença dos mesmos e posterior obtenção da estrutura.

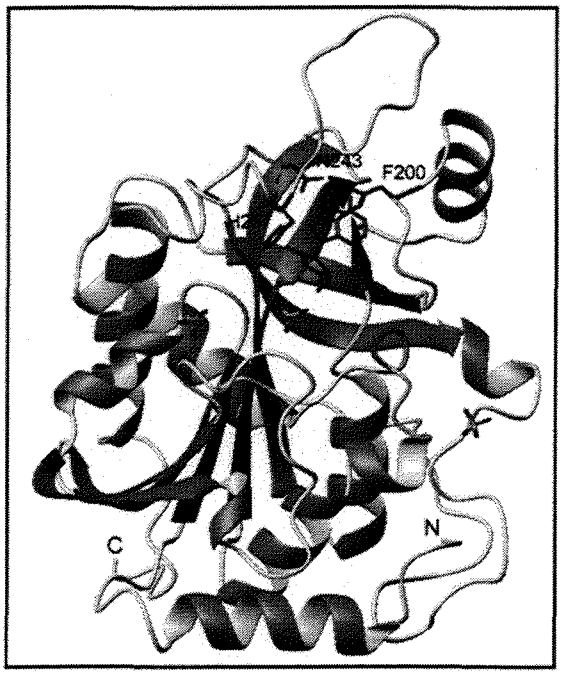

Figura 3: Estrutura tridimensional da PNP humana ligada a inosina e grupamentos sulfato. Alguns dos principais resíduos componentes do sítio de ligação ao nucleosídeo são mostrados, como His257, Asn243 e Phe200. Os átomos de carbono estão representados em cinza, os de nitrogênio, em verde, oxigênio em vermelho e enxofre, amarelo.

A análise em nível atômico tem confirmado, em grande parte, os dados de cinética com formas mutantes da enzima, atribuindo aos resíduos Asn243 e Glu201 funções na catálise e na ligação, respectivamente (Koellner *et al.*, 1997; Mao *et al.*, 1998; Canduri *et al.*, 2004). Os trabalhos mais recentes atualizaram os anteriores, trazendo novas informações que podem auxiliar no desenho de inibidores.

1. 3 Purino nucleosídeo fosforilase e proteção neural

Nos últimos anos, uma série de trabalhos tem ressaltado o envolvimento de nucleosídeos purínicos na modulação neural, bem como sua atuação como neuro-transmissores (Ralevic e Burnstock, 1998; Cunha, 2001; Roesler *et al.*, 2000). Assim, a via de salvamento de purinas tem sido evocada como uma via relevante na patologia de desordens neurais, tais como hipóxia e isquemia (Barsotti, Tozzi e Ipata, 2002; Parkinson *et al.*, 2002; Litsky *et al.*, 1999).

Os nucleosídeos inosina e guanosina são capazes de proteger neurônios e astrócitos contra hipóxia quimicamente induzida (Litsky *et al.*, 1999), bem como células cerebrais sobrevivem, na presença de inosina, a danos causados por zinco (Shi, *et al.*, 2002). Além disso, foi demonstrado que nucleotídeos de adenina e guanina sofrem a ação de nucleotidases, enzimas que hidrolisam nucleotídeos, solúveis em líquido cérebro espinhal de rato, sendo possível uma caracterização cinética aparente dessas enzimas (Portela *et al.*, 2002). Esses resultados enfatizam a importância de nucleosídeos purínicos no metabolismo de células cerebrais submetidas a patologias, tanto agudas quanto crônicas, e outras enzimas da via de salvamento de purinas estão sendo sugeridas como passíveis de desempenhar um papel importante no processo de proteção neural, embora sua atividade ainda não tenha sido diretamente demonstrada em meio extracelular, como as nucleotidases. Assim, para compreender o processo de proteção às células cerebrais por nucleosídeos purínicos, faz-se necessária a aplicação de uma abordagem que investigue a presença de atividade de outras enzimas dessa via, como a purino nucleosídeo fosforilase, em líquido cérebro espinhal.

1. 4 O nucleosídeo sintético 7-metil-6-tio-guanosina

O nucleosídeo artificial 7-metil-6-tio-guanosina (MESG) foi sintetizado como um análogo de guanosina (Webb, 1992), diferindo dessa pela adição de uma metila no átomo N7, o que confere uma carga positiva à base, e pela presença de um átomo de enxofre na posição 6, no lugar do oxigênio (Figura 3). Esse composto passou a ser de grande importância quando foi empregado como substrato em um método de ensaio de PNP bacteriana, uma vez que há uma diferença de absorbância a 360 nm entre MESG e um dos produtos da reação, 7-metil-6-tio-guanina (ε = 11000 M^{-1} cm^{-1}) (Webb, 1992). Desde então, enzimas que liberam P_i em solução têm tido sua atividade medida por um

ensaio acoplado à reação catalisada pela PNP, utilizando MESG como substrato (Oliveira *et al.*, 2003; Wang, Cheng e Killilea, 1995; Nixon *et al.*, 1998). Recentemente, foi demonstrado que a PNP bovina é capaz de hidrolisar MESG na ausência de P_i, como ocorre com inosina, porém um complexo com PNP e 7-metil-6-tio-guanina fortemente ligados não foi verificado (Cheng *et al.*, 1999). Esse substrato também foi utilizado em ensaios para testar inibidores da enzima, visto que permite um método mais simples e rápido do que o ensaio acoplado com a enzima xantina oxidase (Farutin *et al.*, 1999). Uma caracterização cinética da fosforólise de MESG catalisada pela PNP de *Mycobacterium tuberculosis* relatou uma constante de Michaelis (K_M) de 26 μM e uma constante catalítica (k_{cat}) de 49 s^{-1} (Basso *et al.*, 2001).

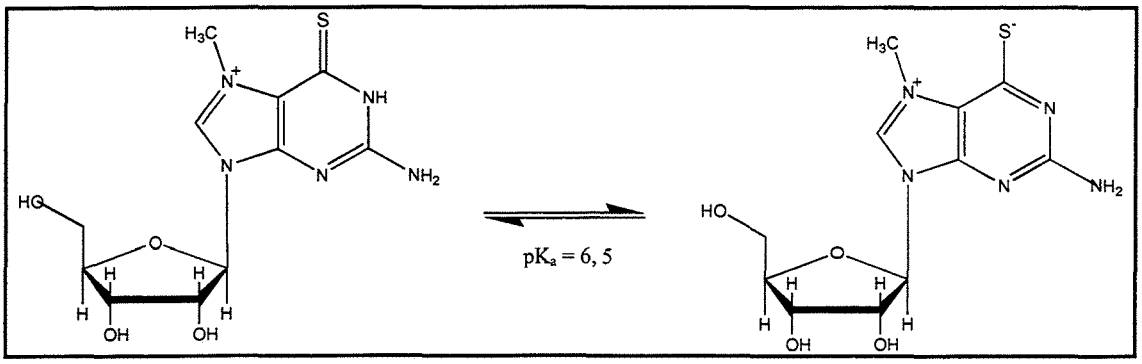

Figura 4: Estrutura molecular do nucleosídeo sintético MESG. Há um equilíbrio entre a forma neutra (à direita) e a positivamente carregada (à esquerda), regido por uma constante de dissociação ácida de 3,16 x 10^{-7} M. A forma que se liga à enzima é, provavelmente, a neutra, pois a enzima é ensaiada, geralmente, em pH 7, 6.

Apesar de sua relevância para o ensaio enzimático de PNP e outras enzimas, não há dados na literatura que descrevam a interação entre MESG e a PNP humana. Assim, o presente trabalho propõe-se a estudar os parâmetros e a natureza dessa interação, tanto cinética quanto estruturalmente, bem como utilizar esse substrato para investigar a presença de atividade de PNP em líquido cérebro espinhal de rato.

2. Objetivos

Os objetivos da linha de pesquisa na qual insere-se o presente trabalho são (*i*) desenvolver inibidores específicos da enzima purino nucleosídeo fosforilase, almejando o tratamento de desordens do sistema imunológico e (*ii*) elucidar o papel desempenhado pela via de catabolismo de purinas no sistema nervoso central.

Em vista disso, este trabalho tem como objetivos gerais analisar as características da interação entre PNP humana e MESG, tanto em solução quanto a nível estrutural, bem como investigar a presença de atividade dessa enzima em líquido cérebro espinhal de rato.

2. 1 Objetivos específicos

2. 1. 1 Verificar, por ensaio enzimático, a presença de atividade de PNP em líquido cérebro espinhal de rato.

2. 1. 2 Determinar as condições de estabilidade da enzima no meio supracitado.

2. 1. 3 Caracterizar cineticamente a enzima, determinando parâmetros como K_M e V (velocidade máxima) aparentes para MESG e P_i.

2. 1. 4 Determinar, por ensaio enzimático em estado estacionário, o mecanismo cinético e parâmetros tais como K_M e K_{cat} da enzima humana para MESG e P_i.

2. 1. 5 Resolver e refinar a estrutura da PNP humana em complexo com MESG e sulfato.

2. 1. 6 Analisar a estrutura, identificando interações importantes para o desenho de inibidores.

3. Artigo 1: Purine nucleoside phosphorylase activity in rat cerebrospinal fluid

Publicado na *Neurochemical Research* em 2004

Neurochemical Research, Vol. 29, No. 10, October 2004 (© 2004), pp. 1831–1835

Purine Nucleoside Phosphorylase Activity in Rat Cerebrospinal Fluid

Rafael Guimarães Silva,[1] Diógenes Santiago Santos,[1,2] Luiz Augusto Basso,[1] Jean Pierre Oses,[3] Susana Wofchuk,[3] Luis Valmor Cruz Portela,[3] and Diogo Onofre Souza[3,4]

(Accepted April 29, 2004)

The sequential hydrolysis of purines is present in rat CSF and generates nucleosides as inosine and guanosine that are usual substrates for purine nucleoside phosphorylase (PNP). PNP catalyzes phosphorolysis of the purine nucleosides and deoxynucleosides releasing purine bases. Here we investigated the presence of PNP in CSF of rats using: i) a specific chromophoric analogue of nucleosides, 2-amino-6-mercapto-7-methylpurine ribonucleoside (MESG), and ii) an inhibitor of PNP activity, immucillin-H. Additionally, we performed a preliminary kinetic characterization (K_M: Henry–Michaelis–Menten constant; V: maximal velocity) for MESG and inorganic phosphate (P_i). The values of K_M and V for MESG (n = 3, mean ± SD) were 142.5 ± 29.5 μM and 0.0102 ± 0.0006 U mg^{-1}, respectively. For P_i (n = 3, mean ± SD), the K_M values and V were 186.8 ± 43.7 μM and 0.0104 ± 0.0016 U mg^{-1}, respectively. The results indicated that PNP is present in rat CSF and provided a preliminary kinetic characterization.

KEY WORDS: CSF; guanosine; inosine; PNP.

INTRODUCTION

The metabolism of purines has been widely studied with particular emphasis for intracellular adenine and guanine-based purines (adenosine, guanosine, inosine, hypoxanthine, xantine, AMP, GMP, ADP, GDP, ATP and GTP). Although their intracellular roles are longer recognized, recently it has been shown their extracellular roles, as can be observed by the roles of ATP (via P_2 receptors) and adenosine (via P_1 receptors) that act as neurotransmitter and neuromodulator respectively, whereas GMP, guanosine and inosine exert neurotrophic and neuroprotective actions (1–6).

Extracellular nucleotides can be hydrolyzed by a variety of enzymes namely NTPDases located on the cell surface or soluble in biological fluids. These enzymes in association with 5'-nucleotidases are involved in the metabolism and control of extracellular nucleotides/nucleosides concentrations, which in consequence result in the modulation of the purinergic signaling (1,7,8). Once formed, the nucleosides can be potentially used as substrate for another family of enzymes called purine nucleoside phosphorylase (PNP) (9,10).

[1] Grupo de Microbiologia Molecular e Funcional, Departamento de Biologia Molecular e Biotecnologia, Instituto de Biociências, Universidade Federal do Rio Grande do Sul, RS, Brazil.
[2] Faculdade de Farmácia, Instituto de Pesquisas Biomédicas Pontifícia Universidade Católica do Rio Grande do Sul, RS, Brazil.
[3] Departamento de Bioquímica, Instituto de Ciências Básicas da Saúde,
[4] Address reprint requests to: Dr. Diogo Onofre Souza, Rua Ramiro Barcelos, 2600, anexo, Porto Alegre, RS, Brazil. Tel: (55) 51 3316 5558; E-mail: diogo@ufgrs.br

PNP is a key enzyme in the purine salvage pathway that catalyzes the reversible phosphorolysis of purine nucleosides, forming purine bases and α-ribose 1-phosphate (9–11). It is specific for purine nucleosides in the beta-configuration and exhibits a preference for ribosyl-containing nucleosides compared to the analogs containing the arabinose, xylose and lyxose stereoisomers (12). The main physiological substrates for mammalian PNP are inosine and guanosine (derived mainly from ribonucleotides hydrolysis), and 2′-deoxyguanosine (from DNA degradation) (9,13).

In humans blood, erythrocytes and T lymphocytes are the richest source of PNP since these cells are deficient in *de novo* synthesis of purines and, consequently, dependent on their salvage synthesis (9,13). Deficiency of PNP is associated with an autosomal recessive form of cellular, but not humoral, immunodeficiency as can be evidenced by the impairment in the T lymphocyte function without considerable interference on B lymphocyte activity (14,15). Clinical manifestations as autoimmune hemolytic anemia and neutropenia, systemic lupus erythematosus, neurologic disorders and B-cell lymphomas are frequently observed in children with PNP deficiency (9,15).

In a previous work we demonstrated the presence of nucleotidase activities in rat cerebrospinal fluid (CSF) that were able to hydrolyze either adenine and guanine nucleotides until nucleosides (16). Moreover, nucleotides, nucleosides and their metabolites are present and were quantified in CSF, as well as the enzyme adenosine deaminase (ADA), which converts adenosine in inosine (17–20). Considering these previous findings, we postulated that PNP activity could be involved in CSF purine metabolism. Accordingly, in the present work we used a specific synthetic substrate to investigate the presence of PNP activity in rat CSF.

EXPERIMENTAL PROCEDURE

Animals and CSF sampling. It was used a total of 190 rats, obtained from our breeding stock, maintained on a 12 h light/12 h dark cycle in a constant temperature (22 ± 1°C) colony room. Free water and a 20% (W/W) protein commercial chow were provided. Animals were separated into three groups, and each group was used in alternate weeks.

The rats were anesthetized with 40 mg kg^{-1} of sodium thiopental, i.p. and CSF was drawn (40–60 μl per rat), by direct puncture of the *cisterna magna* with an insulin syringe (27 gauge 31/20 length). CSF was collected from each rat three or four times (at intervals of 3 weeks), according to our rotative scheme, always in the morning, and CSF samples were pooled (up to 2.0 ml) in a single tube. Individual samples presenting visible blood contamination were discarded. The CSF pool was centrifuged at 4500 × *g* at 5°C for 5 min, to obtain cell-free supernatants.

Purine nucleoside phosphorylase assay. Rat CSF samples were dialyzed against 50 mM Tris–HCl, pH 7.6 for 15 h aiming to remove endogenous inorganic phosphate (P_i) and nucleosides. PNP activity was evaluated in presence of added P_i by the difference between the absorbance of the substrate (2-amino-6-mercapto-7-methylpurine ribonucleoside—MESG) and the product (2-amino-6-mercapto-7-methylpurine base) (21). MESG was obtained from the commercially available Enzchek phosphate assay kit® (Molecular Probes, USA). Incubation time for both substrates (P_i and MESG) varied from 1 to 6 min, the amount of protein varying between 12 and 48 μg mL^{-1}. The reaction gives an absorbance increasing at 360 nm, with an extinction coefficient value of 11,000 M^{-1} cm^{-1} at pH 7.6. Initial steady-state rates were calculated from the linear portion of the time reaction curve for dialyzed rat CSF, in the presence or absence of 1.0 μM Immucillin-H (BioCryst, USA).

Protein determination. Protein concentration was determined by the method of Bradford (22), using the Bio-Rad protein assay kit® (Bio-Rad, USA) and bovine serum albumin as standard.

RESULTS

Rat CSF presents endogenous phosphorolysis activity (PNP activity) on the synthetic substrate MESG, showing a specific activity linear with protein concentration and incubation time (data not shown). The effects of time and temperature of storage on PNP activity were assessed before and after dialysis. Additionally, a preliminary kinetic characterization was performed. The PNP specific activity is expressed as U mg^{-1}, mean ± SD (U = 1 μmol of MESG transformed/min).

For evaluating the influence of temperature (frozen and fresh) on PNP activity, the CSF pool was divided and kept at −20°C or at 4°C. After storage for variable periods the samples were dialyzed and immediately assayed. By keeping the samples for 24 h, a significant loss of PNP activity (80%) was observed in samples kept at −20°C compared to samples kept at 4°C (data not shown). Thus, before the experiments, CSF samples were stored at 4°C.

In order to assess the effect of dialysis on stability of PNP activity, CSF samples were: A) dialyzed immediately after sampling, kept 4°C and assayed after different days; and B) kept 4°C for different days, dialyzed and immediately assayed. The activity remained stable for longer time (5 days) when dialysis was performed immediately after sampling (0.0135 ± 0.0010 U mg^{-1}, n = 3, Fig. 1A). When previously kept for 4°C for different days before the dialysis, the activity (measured

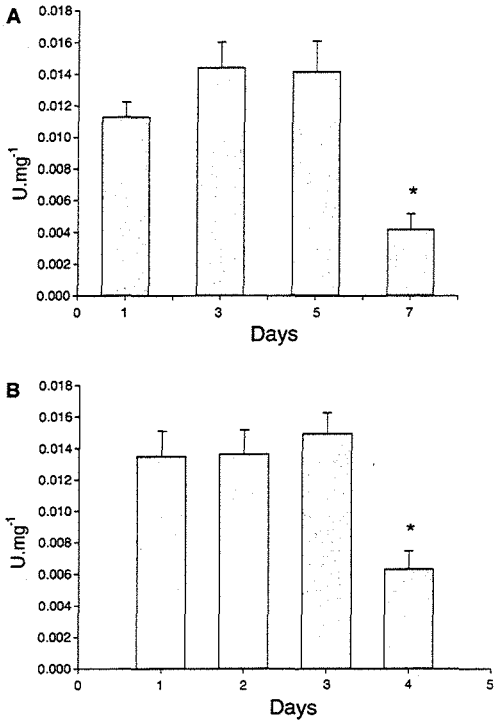

Fig. 1. Effect of time storage of CSF before/after dialysis on the stability of PNP activity. (A) CSF was dialyzed immediately after sampling, stored at 4°C for different days and assayed, or (B) CSF was stored at 4°C for different days, dialyzed and immediately assayed. In the 7th day in A, and in 4th day in B there was a significant decrease of PNP activity, at $*P < 0.05$, by Student "t" test.

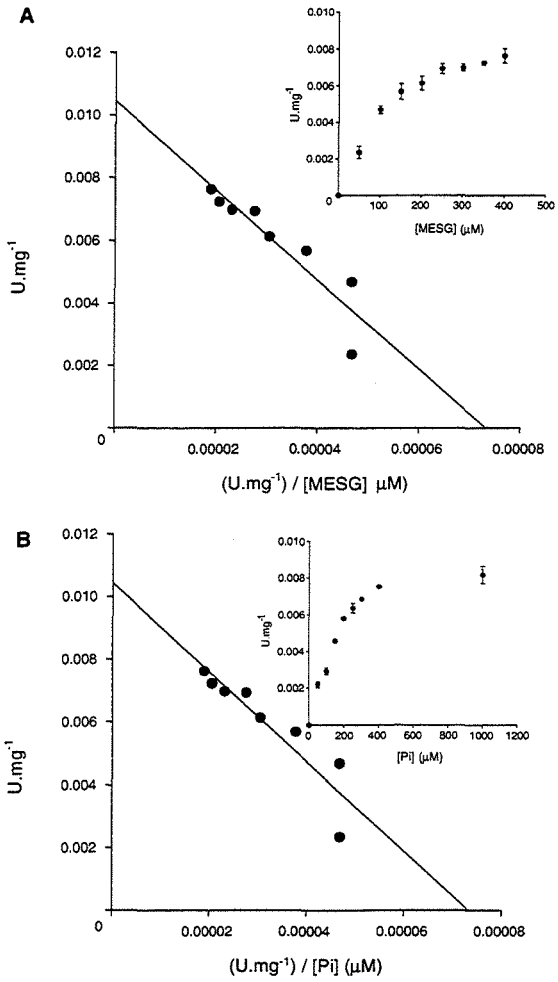

Fig. 2. Apparent kinetic parameters (K_M: Henry–Michaelis–Menten constant; V: maximal velocity) were evaluated for PNP, varying MESG (200 µM P_i, n = 3) and P_i (200 µM MESG, n = 3) concentrations and were estimated by Eadie-Hofstee plot. Apparent K_M and V for MESG were 142.5 ± 29.5 µM and 0.0102 ± 0.0006 U mg^{-1} respectively (A). Apparent K_M and V for P_i were 186.8 ± 43.7 µM and 0.0104 ± 0.0016 U mg^{-1}, respectively (B). Saturation curves for MESG and P_i are showed as insert.

immediately after dialysis) was stable for 3 days (0.0160 ± 0.0015 U mg^{-1}, n = 3, Fig. 1B). Thus, in further experiments CSF samples were dialyzed immediately after sampling before storage at 4°C. Protein concentration varied in all CSF samples from 0.10 to 0.14 mg ml^{-1}.

In order to preliminary evaluate the specificity of phosphorolysis activity, concerning the PNP activity, we tested the effect of 1 µM immucillin-H, which is a powerful and selective PNP inhibitor (23). The phosphorolysis activity (0.0174 ± 0.0067 U mg^{-1}, n = 3) was completely abolished by immucillin-H, strongly suggesting that the activity was specifically due to PNP activity.

The apparent steady-state kinetic parameters (K_M = Henry-Michaelis-Menten constant, V = maximal velocity) were determined for MESG and inorganic phosphate. The apparent K_M and V for MESG were determined varying MESG concentration (50 to 400 µM) at a fixed P_i concentration (200 µM). The apparent K_M and V for P_i were determined varying P_i concentration (50 to 1000 µM) at fixed MESG concentration (200 µM). Both determinations were carried out using 24 µg mL^{-1} protein (final concentration). The values of K_M and V for MESG were 142.5 ± 29.5 µM and 0.0102 ± 0.0006 U mg^{-1} (n = 3) respectively (Fig. 2A); the values of K_M and V for P_i were 186.8 ± 43.7 µM and 0.0104 ± 0.0016 U mg^{-1} (n = 3), respectively (Fig. 2B).

DISCUSSION

Extracellular inosine and guanosine, generated by the sequential breakdown of purines or released from neural cells, have been implicated in neuroprotective processes against glutamatergic toxicity. Indeed, our group has shown that guanosine prevents seizures induced by over stimulation of the glutamatergic system (quinolinic acid or α-dendrotoxin) (2,5,6), whereas guanosine and inosine preserve both neuronal and glial cell viability during chemical hypoxia, and metal-induced injury (3,24–26). It is known that various purine derivatives are present in CSF, probably due to their intracellular release and/or to sequential action of different enzymatic systems (16,20). Here we reported the presence in rat CSF of PNP activity, a key enzyme of purine salvage pathway, which was totally inhibited by Immucillin-H, a specific PNP activity inhibitor. This finding could be relevant for clinical studies where PNP activity could be investigated as possible marker of pathological brain states. The simultaneous occurrence of absence or low levels of PNP and neurological disorders strongly supports diagnosis of PNP immunodeficiency. Low PNP levels and high ADA/PNP ratio were observed in various types of leukemia and lymphoma, as well as the ADA/PNP ratio seems to reflect the clinical severity (9). Thus, determination of PNP in CSF of humans appears to be an attractive tool for investigating brain disturbs involving purine metabolism in CNS.

Concerning to methodological approach here used, CSF contaminated with blood was discarded to avoid erythrocytes and leucocytes source of PNP activity. Moreover, the dialysis allowed eliminate endogenous nucleosides and Pi that could interfere with PNP activity assay (27). The effect of storage was verified in order to evaluate the stability of PNP activity pos sampling for future studies involving human CSF samples.

Compared to previous values reported for intracellular PNP activity, in the present work we found about 3-fold higher apparent K_M and lower apparent V_{max} for both MESG and P_i. Although at the moment the physiological relevance of these findings are not clear, we postulate that this high K_M could contribute to the neuroprotective and neuromodulatory effects of extracellular nucleosides guanosine and inosine (3,5). If true, in neurological insults where increased concentrations of purines and glutamate is observed, the high K_M of PNP becomes favorable for the maintenance of neuroprotective nucleosides action on neural cells.

Here we reported for the first time the presence of PNP activity in rat CSF, as well as some preliminary evaluation of apparent kinetic parameters; some methodological parameters were also presented. The physio/pathological relevance of PNP activity in CSF remains to be clarified.

ACKNOWLEDGMENTS

Financial support for this work was provided by Millenium Initiative Program MCT-CNPq, Ministry of Health—Secretary of Health Policy (Brazil) to D.S.S. and L.A.B. D. S.S. and L.A.B. also acknowledge grants awarded by CNP*q* and FINEP, and J. P.O. is supported by CAPES. We would also like to thank Shanta Bantia (BioCryst Pharmaceuticals Inc., Birmingham, Al) for the generous gift of immucillin-H.

REFERENCES

1. Burnstock, G. 2002. Purinergic signaling and vascular cell proliferation and death. Arterioscler Thromb Vasc Biol. 22:364–373.
2. Lara, D. R., Schmidt, A. P., Frizzo, M. E., Burgos, J. S., Ramirez G., and Souza D. O. 2001. Effect of orally administered guanosine on seizures and death induced by glutamatergic agents. Brain Res. 912:176–180.
3. Litsky, M. L., Hohl, C. M., Lucas, J. H., and Jurkowitz, M. S. 1999. Inosine and guanosine preserve neuronal and glial cell viability in mouse spinal cord cultures during chemical hypoxia. Brain Res. 821: 426–432.
4. Rathbone, M. P., Middlemiss, P. J., Gysbers, J. W., Andrew, C., Herman, M. A.R., Reed, J. K., Ciccarelli, R., Di Iorio P., and Caciagli, F. 1999. Trophic effects of purines in neurons and glial cells. Prog. Neurobiol. 59:663–690.
5. Schmidt, A. P., Lara, D. R., Maraschin, J. F., Perla, A. S., and Souza, D. O. 2000. Guanosine and GMP prevent seizures induced by quinolinic acid in mice. Brain Res. 864:40–43.
6. Vinadé, E. R., Schmidt, A. P., Frizzo, M. E., Izquierdo, I., Elisabetsky E., and Souza, D. O. 2003.Chronically administered guanosine is a aoticonvumsant, amnesic and anxiolytic in mice. Brain Res. 977:97–102.
7. Cunha, R. A. 2001.Regulation of the ecto-nucleotidase pathway in rat hippocampal nerve terminals. Neurochem. Res. 26:979–991.
8. Zimmermann, H. 2001. Ectonucleotidases: Some recent developments and a note on nomenclature. Drug. Dev. Res. 52:44–56.
9. Bzowska, A., Kulikowska, E., and Shugar, D. 2000. Purine nucleoside phosphorylases: properties, functions, and clinical aspects. Pharmacol. Ther. 88:349–42.
10. Bzowska, A., Luic, M., Schroder, W., Shugar, D., Saenger, W., and Koellner, G. 1995. Calf spleen purine nucleoside phosphorylase: purification, sequence and crystal structure of its complex with an N(7)-acycloguanosine inhibitor. FEBS Lett. 367:214–218.
11. Parks Jr. R. E., and Agarwal, R. P. 1972. The enzymes, Vol. 7. Pages 483—514, in Boyer, P. D. (ed.), Academic Press, New York.

12. Stoeckler, J. D., Cambor., C. and Parks Jr. R. E. 1980. Human erythrocytic purine nucleoside phosphorylase: reaction with sugar-modified nucleosides substrates. Biochemistry. 19:102–107.
13. Stoeckler, J. D. 1984. Developments in Cancer Chemotherapy. Pages 35–6 Glazer, R. I. (ed.), CRC Press, Bocca Raton, FL.
14. Giblett, E. R., Ammann, A. J., Wara, D. W., Sandman. R., and Diamond, L. K. 1975. Nucleoside-phosphorylase deficieocy in a child with severely defective T-cell immunity and normal B-cell immunity. Lancet. 1:1010–1013.
15. Hershfield, M. S. and Mitchell, B. S. (1995). Immunodeficiency diseases caused by adenosine deaminase deficiency and purine nucleoside phosphorylase deficiency. Pages 1725—1768, in Scriver C. R., Beaudet A. L., Sly W. S., and Valle D. (eds.), The metabolic and molecular bases of inherited disease. McGraw-Hill, New York.
16. Portela, L. V. C., Oses, J. P., Silveira, A. L., Schmidt, A. P., Lara, D. R., Battastini, A. M.O., Ramirez, G., Vinadé, L., Sarkis, J. J.F., and Souza, D. O. 2002. Guanine and adenine nucleotidase activities in rat cerebrospinal fluid. Brain Res. 950:74–78.
17. Rodríguez-Nuñez, A., Camina, F., Lojo, S., Rodríguez-Segade, S., and Castro-Gago, M. 1993. Concentrations of nucleotides, nucleosides, purine bases and urate in cerebrospinal fluid of children with meningitis. Acta Paediatr. 82:849–852.
18. Rodríguez-Nuñez, A., Cid, E., Rodríguez-Garcia, J., Camina, F., Rodriguez-Segade, S., and Castro-Gago, M. 2000. Cerebrospinal fluid purine metabolite and neuron-specific enolase concentrations after febrile seizures. Brain Dev. 22:427–431.
19. Rodriguez-Nunez, A., Cid, E., Rodriguez-Garcia, J., Camina, F., Rodriguez-Segade, S., and Castro-Gago M. 2003. Neuron-specific enolase, nucleotides, nucleosides, purine bases, oxypurines and uric acid concentrations in cerebrospinal fluid of children with meningitis. Brain Dev. 25:102–6.
20. Choi, S. H., Kim, Y. S., Bae, I. G., Chung, J. W., Lee, M. S., Kang, J. M., Ryu, J., and Woo, J. H. 2002. The possible role of cerebrospinal fluid adenosine deaminase activity in the diagnosis of tuberculous meningitis in adults. Clin. Neurol Neurosurg. 104:10–5.
21. Webb, M. R. 1992. A continuous spectrofotometric assay for inorganic phosphate and for measuring phosphate release kinetics in biological systems. Proc. Natl. Acad. Sci. U.S.A. 89:4884–4887.
22. Bradford, M. M. 1976. A rapid and sensitive method for the quantification of microgram quantities of protein utilizing the principle of protein-dye binding. Anal. Biochem. 72:218–254.
23. Horenstein, B. A. and Schramm, V. L. 1993. Correlation of the molecular eletrostatic potential surface of an enzymatic transition state with novel transition-state inhibitors. Biochemistry 32:9917–9925.
24. Frizzo, M. E., Lara, D. R., Prokopiuk, A. S., Vargas, C. R., Salbego, C. G., Wajner, M., and Souza, D. O. 2002. Guanosine enhances glutamate uptake in brain cortical slices at normal and excitotoxic conditions. Cell Mol. Neurobiol. 22:353–363.
25. Shi, M., You, S. W., Meng, J. H., and Ju, G. 2002. Direct protection of inosine on PC12 cells against zinc-induced injury. NeuroReport 13:477–479.
26. Jurkowitz, M. S., Litsky, M. L., Browning, M. J., and Hohl C. M. 1998. Adenosine, inosine, and guanosine protect glial cells during glucose deprivation and mitochondrial inhibition: correlation between protection and ATP preservation. J. Neurochem. 71:535–548.
27. Ropp, P. A. and Traut, T. W. 1991. Allosteric regulation of purine nucleoside phosphorylase. Arch. Biochem. Biophys. 288:614–620.

4. Artigo 2: Crystal structure and kinetics of human purine nucleoside phosphorylase in complex with 7-methyl-6-thio-guanosine

Submetido ao *Journal of Biological Chemistry*

CRYSTAL STRUCTURE AND KINETICS OF HUMAN PURINE NUCLEOSIDE PHOSPHORYLASE IN COMPLEX WITH 7-METHYL-6-THIO-GUANOSINE*

Rafael G. Silva[1], José H. Pereira[2], Fernanda Canduri[2], Walter F. de Azevedo Jr.[2], Luiz A. Basso[3], and Diógenes S. Santos[1]

[1]Centro de Pesquisas em Biologia Molecular e Funcional, Instituto de Pesquisas Biomédicas, Pontifícia Universidade Católica do Rio Grande do Sul, Porto Alegre, RS, Brazil.

[2]Departamento de Física, UNESP, São José do Rio Preto, SP, Brazil.

[3]Departamento de Biologia Molecular e Biotecnologia, Universidade Federal do Rio Grande do Sul, Porto Alegre, RS, Brazil.

Running Title: Structure and kinetics of human PNP complexed with MESG

Address correspondence to: Diógenes S. Santos or Luiz A. Basso, Centro de Pesquisas em Biologia Molecular e Funcional, Instituto de Pesquisas Biomédicas, Pontifícia Universidade Católica do Rio Grande do Sul, 6681/92-A Av. Ipiranga, 90619-900, Porto Alegre, RS, Brazil. Phone/Fax: +55 51 33203629. E-mails: diogenes@pucrs.br or labasso@cbiot.ufrgs.br .

Purine nucleoside phosphorylase catalyzes the reversible phosphorolysis of nucleosides and deoxynucleosides, generating the ribose 1-phosphate and the purine base. It is an important step of purine catabolism pathway. The lack of such an activity in humans, owing to a genetic disorder, causes T-cell impairment, and drugs that inhibit this enzyme may have the potential of being utilized as modulators of the immunological system to treat leukemia, autoimmune diseases, and rejection in organ transplantation. Here we describe kinetics and crystal structure of human purine nucleoside phosphorylase in complex with 7-methyl-6-thio-guanosine, a synthetic substrate, which is largely used for enzymatic activity assays. Analysis of the structure identifies different conformational changes on the enzyme upon ligand binding, and comparison of kinetic and structural data permits the understanding of effects of atomic substitution on key positions of the synthetic substrate molecule and their consequences to enzyme binding and catalysis. Such knowledge may be helpful in designing new PNP inhibitors.

Purine nucleoside phosphorylase (PNP)[1] (EC 2.4.2.1) is a key enzyme of the purine salvage pathway, responsible for the inter-conversion between (deoxy)nucleosides and bases, which in turn may be converted to uric acid for excretion or reused in nucleic acid biosynthesis [1]. This enzyme catalyzes the reversible cleavage, in the presence of inorganic phosphate (P_i), of *N*-ribosidic bonds of purine nucleosides and deoxynucleosides, except adenosine, to generate ribose 1-phosphate and the corresponding purine base [2]. The reaction proceeds with inversion of configuration, from α-nucleosides to β-ribose 1-phosphate [3].

Human PNP (HsPNP) is classified, based on substrate specificity and structural characteristics, into the Nucleoside Phosphorylase-I family, which includes nucleoside phosphorylases with either trimeric or hexameric quaternary structure and a common single-domain subunit, accepting both purine and pyrimidine nucleosides as substrates [4]. Interest in this enzyme has been greatly increased since the discovery that the congenital absence of its activity causes T-cell impairment in human beings, though keeping normal levels of B-cells [5, 6]. Hence, HsPNP has being proposed as a target for drug design, aiming the enzyme inhibition for treatment of immunological disorders [7]. Several studies, involving kinetic and structural characterization of the enzyme with a range of substrates have been carried out to elucidate its mechanism and to help develop potent inhibitors, suggesting great importance of N7, N1, and O6 positions of substrates and Glu201 and Asn243 side chains of enzyme for substrate binding and catalysis [8-15].

In the work presented here, X-ray diffraction crystallography and steady-state kinetics were utilized to study the interaction

between recombinant HsPNP and 7-methyl-6-thio-guanosine (MESG) (Fig. 1), a guanosine analogue largely employed in PNP activity assay and dosage of P_i in solution [16-19]. The results reported here describe the differences in HsPNP active site and MESG interaction as compared to natural substrates, which should help understand the effects on ligand binding and catalysis of chemical substitutions on key positions of the substrate molecule. It is hoped that this knowledge will aid the development of new and more powerful HsPNP inhibitors with therapeutic activity.

MATERIALS AND METHODS

Crystallization and Data Collection - Recombinant human PNP was obtained as previously described [20]. A solution of 11 mg mL^{-1} HsPNP in 20 mM Tris-HCl pH 7.6 was incubated in the presence of 0.6 mM MESG (Molecular Probes). Hanging drops were equilibrated by vapor diffusion at 16° C against reservoir containing 21% (v/v) saturated ammonium sulfate solution in 50 mM citrate buffer (pH 5.3).

In order to increase the resolution of the HsPNP:MESG crystals, data were collected from a flash-cooled crystal at 104 K. Prior to flash-cooling, glycerol was added to the crystallization drop up to 50% by volume. X-ray diffraction data were collected at 1.431 Å using the Synchrotron Radiation Source (Station PCr, Laboratório Nacional de Luz Síncrotron, Campinas, Brazil) and a CCD detector (MARCCD) with an exposure time of 100 s per image at a distance from crystal to detector of 130 mm. X-ray diffraction data were processed to 2.8 Å resolution using the program MOSFLM and scaled with the program SCALA [21].

Structure Resolution and Refinement - The crystal structure of HsPNP:MESG was determined by molecular replacement methods, using the program AMoRe [22], with HsPNP:acyclovir[2] [23] as search model, with ligand and water removed. Structure refinement was performed using X-PLOR [24], and atomic positions from molecular replacement were used to initiate refinement. The stereochemistry of the final structure for HsPNP:MESG complex[3] was checked by the program PROCHECK [25]. Superposition was performed with Swiss-PDB-Viewer [26].

Kinetic Analysis - Recombinant HsPNP was assayed in the forward direction in 50 mM Tris-HCl, pH 7.6. Enzyme activity was measured by the difference in absorbance between 7-methyl-6-thio-guanosine and the purine base product of its reaction with inorganic phosphate catalyzed by PNP [16]. This reaction gives an absorbance increase at 360 nm with an extinction coefficient value of 11,000 M^{-1} cm^{-1} at pH 7.6 [16]. Initial steady-state rates were calculated from the linear portion of reaction curves obtained by varying MESG concentration (10 μM – 500 μM) against several varied-fixed P_i concentrations (10 μM – 1600 μM), and vice-versa. Lineweaver-Burk plots were constructed against $[MESG]^{-1}$ and $[P_i]^{-1}$, and the intercepts calculated for each fixed concentration of the second substrate. The y-axis intercepts from double-reciprocal plots for P_i plotted against $[MESG]^{-1}$ must yield straight lines [27, 28] defined, respectively, by

$$1/V_{app} = (\alpha K_{MESG}/V \times [MESG]^{-1}) + 1/V \quad (1),$$

where V_{app} values are the y-axis intercepts from double-reciprocal plots for P_i as the varied-fixed substrate, K_{MESG} is the K_m (Michaelis constant) for MESG, V is the maximal velocity of the reaction, and α is a factor that represents the influence of $[P_i]$ on the affinity of the enzyme for MESG. The same procedure was applied to intercepts from double-reciprocal plots for MESG, yielding straight lines obeying the following equation:

$$1/V_{app} = (\alpha K_{Pi}/V \times [P_i]^{-1}) + 1/V \quad (2),$$

where V_{app} values are the y-axis intercepts from double-reciprocal plots for MESG as the varied-fixed substrate, K_{Pi} is the K_m for P_i, V is the maximal velocity of the reaction, and α is a factor that represents the influence of [MESG] on the affinity of the enzyme for P_i.

RESULTS

Reaction of purine nucleoside phosphorylase with MESG and P_i has been utilized in coupled-assays to assess several enzymatic activities that release P_i in solution [16-19], and to assay and characterize PNP activity from various sources [16, 20, 29, 30]. In order to acquire a better understanding of the interaction between human PNP and ligands, steady-state kinetic parameters for HsPNP-catalyzed phosphorolysis of MESG were determined. For both substrates, saturation of the enzyme was reached (Fig. 2A and Fig. 3A), and the pattern of linear double-reciprocal plots indicate a sequential addition of substrates to the enzyme (Fig. 2B and Fig. 3B). Fitting the data to equations 1 and 2 yielded a K_m value of 358 μM for MESG (Table I), a value at least 20-fold higher than those previously reported for natural substrates and 7-methyl-guanosine [31-33]. Affinity of HsPNP for P_i seemed not to be altered in the presence of MESG in comparison to other substrates, since the K_m value found for this substrate was 94 μM (Table I), in agreement with the literature [3, 7, 33, 34]. Moreover, the family of double-reciprocal plots (Fig. 2B and Fig. 3B) intersect on the x-axis indicating that binding of one ligand does not change the affinity for the second ligand. A value of 40 s^{-1} was found for the catalytic constant (k_{cat}), which is similar to that for phosphorolysis of inosine by human erythrocyte PNP [31]. Thus, MESG, with a specificity constant of 1.1 x 10^5 M^{-1} s^{-1}, is shown to be a less specific HsPNP substrate in comparison with inosine, guanosine, and deoxyguanosine, and this effect is due to a loss in binding affinity, since catalysis is unchanged.

To try to evaluate the probable interactions that are responsible for the differing kinetic parameter for HsPNP with MESG as compared to those for other nucleosides, crystal structure of HsPNP in complex with MESG was determined at 2.8 Å resolution. Parameters of data collection, refinement statistics, and structure quality are summarized in Table II. The HsPNP:MESG complex displays a trimeric structure, as expected based on previously reported structures for this enzyme with different ligands [9, 13-15, 23]. The monomer consists of internal β-sheets, forming a distorted β-barrel, surrounded by α-helices. Although the superposition of HsPNP:MESG structure on the apoenzyme[4], in the Cα coordinates, generated a modest r.m.s deviation of 1.15 Å, there are some observable conformational changes in the secondary structure of the enzyme upon ligand binding. The α-helix formed by residues Ala262-Ala280 in the apoenzyme is shorter in the HsPNP:MESG complex, involving residues Ala267-Ser281. The opposite occurs with the α-helix formed by Thr97-Leu105 residues in the HsPNP:MESG complex, since this helix is shorter in the apoenzyme structure, consisting of residues Pro99-Phe103 (Fig. 4A and B). A change from coil to helix involving residues His257-Lys265 in the transition of apoenzyme to ligand-bound enzyme species, reported for crystal structures of HsPNP with various substrates and inhibitors [14, 15, 23, 35, 36], was not observed in the present structure (Fig. 4B).

Differences in the position of amino acid side chains were also observed in the enzyme active site of the HsPNP:MESG structure. The side chain of His257 lies in a different position in relation to HsPNP in complexes with inosine (HsPNP:Ino) and 2'-3'-dideoxyinosine (HsPNP:ddI) [15], and it is probably not interacting, through hydrogen bond, with the ribose moiety of MESG (Fig. 5A-C). The side chain of Asn243 is more distant from the N7 position of MESG as compared to HsPNP:Ino and HsPNP:ddI (Fig. 5A-C), but is in a similar location as compared to HsPNP:immucillin-H complex structure (HsPNP:ImmH) [35]. The phenyl ring of Phe200 occupies the same position in HsPNP:MESG, HsPNP:Ino, and HsPNP:ddI structures (Fig. 5A-C), indicating that the hydrophobic interactions between this residue and the purine base, shown to be essential for both catalysis and substrate binding [31], were not affected by the chemical substitutions present in MESG.

The hydrogen bond (H-bond) pattern between HsPNP and MESG changed when compared to other ligands. Interactions between Asn243 and ligands are conserved in all human and bovine PNP (bPNP) structures reported so far [8, 14, 15, 23, 35, 36-41], as well as in the structure of *Mycobacterium tuberculosis* complexed with ImmH, where the Asn231 plays a similar role [42]. In the present structure, the carbonyl group of

Asn243 is at 3.3 Å from the positively charged N7 of MESG and participate in an ion-dipole electrostatic interaction (Fig. 6). This type of interaction is in contrast to those observed for the complexes of HsPNP with guanine, inosine, and ImmH [14, 15, 35]. The amino group of Asn243 is at 3.7 Å from the S6 of MESG (Fig. 6), a value larger than the 3.5 Å cutoff generally accepted to assign hydrogen bonds, and whether this interaction actually exists or not in HsPNP:MESG complex is uncertain. The H-bond between HsPNP Glu201 side chain and N1, essential for both substrate binding and catalysis [31], is also weaker in the HsPNP:MESG as compared to the HsPNP complexes with guanine, ImmH, hypoxanthine [14, 34, 36] and bPNP complexes with ImmH and immucillin-G (ImmG) [37, 41]. The bidentate carboxylate group of Glu201 more closely contacts MESG through a 2.7 Å H-bond with the amino group on N2 of the guanosine analogue (Fig. 6). Concerning to the ribose sub-site, the most relevant interactions are those involving the main chain nitrogen of Met219 and the hydroxyl group of Tyr88 with O2' and O3' of the ribose, respectively, and that between sulfate group O1 and ribose O3', characterized by a 2.7 Å H-bond (Fig 6). It is noteworthy that a water molecule is hydrogen-bonded to 5'- hydroxyl group of MESG, which may be important, since, in the present structure, the imidazole ring of His257 is not oriented to interact with 5'-hydroxyl group of the substrate (Fig. 5A), in contrast to what is observed for several structures of PNP with ligands [15, 35, 37, 40, 41]. The 5'-OH group of MESG seems to adopt an unfavorable syn configuration, as in the structures of bovine and human PNPs with ImmH, a transition state analog that is a potent PNP inhibitor [35, 41]. However, since this portion of the substrate showed high temperature factors (~60 $Å^2$), weak electron density was seen for the 5'-oxygen, and its configuration cannot be reliably assigned.

DISCUSSION

The rational design of inhibitors is dependent upon knowledge of interactions at the atomic level between enzyme and its ligand molecules. HsPNP is proposed as a drug target for the development of modulators of the immunological system and the rational design of inhibitors of this enzyme has employed kinetic and structural investigations [8-15]. Study of PNP-catalyzed cleavage of the *N*-ribosidic bond of 7-methyl-6-thio-guanosine allows assessment of the effects on reaction parameters caused by modifications on substrate molecule. The mechanism of catalysis proposed for bPNP, based on analysis of kinetic isotope effects, implies the protonation of the base, with oxocarbenium ion character development on the ribose moiety when reaction reaches its transition state [10-12]. Protonation of the base is also supported by acid-catalyzed *N*-ribosidic bond cleavage of purine nucleosides, while reaction rates for 7-methyl-guanosine, which is already protonated, are pH-independent [43]. The N7-subtituted purine nucleosides develop a positive charge on the purine ring and would have labile C1-N9 bonds. Interestingly, the methyl group substitution on N7 of MESG does not have any effect on k_{cat} value since it is similar to those found for HsPNP-catalyzed phosphorolysis of natural substrates [31]. Considering that there are two forms of MESG in solution (pK_a = 6.5), the form with neutral net charge (Fig. 1) is predominant in solution at pH 7.6, and it is likely that this is the form of MESG that binds to the enzyme in the assay conditions. Hence, the *N*-ribosidic bond would not be any weaker than that of natural substrates, explaining the similar k_{cat} values for MESG and inosine [31]. The K_m for MESG is 20-fold larger than those for guanosine and 7-alkyl-guanosine analogues [33, 44]. The K_m for N7-substituted substrates of PNP are not expected to be larger than those for the non-substituted ones, as indicated by theoretical and experimental studies on the free energies for binding of N7-alkylated guanosines to bPNP, even when the alkyl groups were bulkier than the methyl radical [32]. Thus the loss in affinity of HsPNP for MESG is probably due to the replacement of oxygen by sulfur at the sixth position of the purine base. Interestingly, data reported for a series of competitive inhibitors of bPNP indicated that inhibitors displayed lower K_i (inhibition constant) values when MESG was the substrate, relative to those with inosine as substrate [45].

It is noteworthy that kinetic curves for P_i presented here, with various concentrations of MESG as co-substrate, are

hyperbolic (Fig. 2A and 3A) and can be described by the Michaelis-Menten equation. This is in contrast to data reporting non-linear kinetics and allosteric regulation of PNP with phosphate [3, 46], but is in agreement with the results observed when 7-methyl-guanosine was the second substrate [33]. Concerning to the enzyme kinetic mechanism with MESG, steady-state kinetics results indicate that the substrates bind to the enzyme in a sequential order and binding of one substrate does not change the affinity of the second substrate (α = 1). In addition, the linearity of double-reciprocal plots at all substrate concentrations indicates that a steady-state random mechanism can be discarded [28]. A rapid-equilibrium random mechanism appears to describe the phosphorolysis of MESG catalyzed by HsPNP, even though a steady-state ordered mechanism cannot be discarded. An ordered Bi – Bi reaction was proposed for human erythrocyte PNP, on the basis of product inhibition experiments, with the nucleoside binding first [47], whereas the opposite was found for bPNP, with P_i being the first substrate to be added to the enzyme [3]. Both data should be interpreted carefully, since it was shown that bPNP can hydrolyze inosine [10] and MESG [48] in the absence of P_i. In addition, crystal structures of erythrocyte and recombinant human PNP have been reported with sulfate groups bound in the phosphate-binding site, with no nucleoside present, and conformational changes in the enzyme that could represent a hindrance to the binding of the nucleoside were not observed [9, 13].

From the structural viewpoint, no major differences in the overall arrangement is observed in the present structure, compared to those reported earlier for HsPNP bound to various molecules, except that the latter ones undergo a coil-to-helical transformation, involving residues around His257, upon binding of inhibitors or substrates [8, 14, 15, 23, 35, 36] as compared to the apoenzyme structure [9, 13]. This coil-to-helical transformation is not observed in the HsPNP:MESG structure. Movements involving active site residue side chains reflect a diversity in the mode of binding of HsPNP with its substrates. A water molecule makes contact to 5'-OH group of MESG (Fig. 6), and the side chain of His257 is not positioned to interact with substrate (Fig. 5A), an observation in striking contrast to those reported for all structures of both bovine and human PNPs in complex with ligands containing a ribose ring in their structures [15, 35, 37, 40, 41]. Although the hydrogen bond between His257 and 5' position of inosine has been suggested to play a minor role in binding affinity [31], 5'-deoxy-immucillin-H showed a 1000-fold increase in K_i in comparison to immucillin-H [37]. So, it is possible to conclude that the 5'-OH group is of capital importance for nucleosides to interact with PNP, but this interaction can be mediated by an active site water molecule instead of His257.

The side chain of Asn243 is also in a different position relative to the structures of HsPNP in complex with inosine, ddI, and acyclovir [15, 23,]. In the latter structures, the side chain carboxamide group of Asn243 is positioned to donate an H-bond to both N7 and O6 atoms of the ligand molecules, whereas in the HsPNP:MESG structure the carbonyl group of Asn243 forms an ion-dipole electrostatic interaction with the positively charged N7. It has been proposed that Asn243 side chain has enough mobility to relocate away from the active site when activation of the nucleoside is not necessary [40, 49]. However, Asn243 in the HsPNP:MESG structure is at a distance (3.3 Å) suitable to form the ion-dipole interaction with N7 of substrate, even though a methyl group is anchored at this position. Although this residue is thought to have little effect on binding [31], the interaction cited above may be important for MESG; otherwise Asn243 would not contact the substrate because the H-bond with S6 is probably not present. The only reported structure of a trimeric PNP in which Asn246 (Asn243 in human and bovine PNPs) does not interact directly with substrate is that of *Cellulomonas sp.* enzyme, where a water molecule mediates this interaction [50]. Such water molecule is not observed in the present structure, and the electrostatic interaction between N7 and Asn243 seems to be the only contact between this residue and the substrate. The lower affinity of HsPNP for MESG, in comparison to other substrates, may be explained by a lack of H-bond between Asn243 and S6 of the substrate. Weak hydrogen bonds (> 2.8 Å) are reported to have activation energies of 1-3 kcal/mol in aqueous and aqueous-acetone

solutions [51], and this type of interaction is found for Asn243 with O6 of inosine in both human and bovine enzyme Michaelis complexes [15, 40]. A large loss of binding affinity was observed for bPNP and 6-thio-ImmH, compared to that for ImmH, and it was attributed to the lack of two H-bonds around O6 [37]. Here, only one hydrogen bond is missing in the sixth position of substrate, and this can readily account for the 1.9 kcal/mol decrease in stability of the Michaelis complex of HsPNP and MESG, relative to that with inosine, guanosine, and 7-methyl-guanosine.

Interaction between Glu201 and inosine has been shown to be essential for both binding and catalysis [31], and it is present in other complexes of trimeric PNPs with substrates or inhibitors, for instance, in bPNP:hypoxanthine [39], *Mycobacterium tuberculosis* PNP (Glu189) in complex with ImmH [42], and *Cellulomonas sp.* PNP (Glu204) with 8-iodo-guanine, where this residue was proposed to play the key role in the mechanism of catalysis, instead of Asn246 [50]. In the present structure, Glu201 is the only residue that participates of a strong H-bond (2.7 Å) with MESG, since other H-bonds are present at greater distance values (Fig. 6). However, Glu201 is hydrogen-bonded to the amino group on N2 and, since the K_m for inosine and guanosine are similar, interaction at this position probably plays no role in the affinity of HsPNP for MESG.

In the phosphate-binding site, contacts involving sulfate group and enzyme do not differ appreciably from those of other structures of HsPNP with ligands [15, 23, 35]. It should be pointed out, however, that the distance separating sulfate group from O4' of MESG is 3.3 Å, a value somewhat shorter than that between sulfate and O4' of inosine (3.6 Å) in the bPNP:inosine:sulfate ternary complex [40], and larger than that of phosphate and N4' of ImmH (2.8 Å) in bPNP:immucillin-H:phosphate ternary complex [41]. Approximation between phosphate and nucleoside is proposed to be due to electrostatic attraction between negative oxygen of phosphate and the partial positive charge developed on the ribose moiety when reaction reaches its transition state [41]. As this approximation is necessary to ensure the bond formation between ribose C1' and a phosphate oxygen, the present structure may represent a snapshot capturing the atomic motion that occurs during the course of the reaction.

The work presented here describes the kinetic parameters and structural interactions at atomic level between recombinant human PNP and 7-methyl-6-thio-guanosine. To the best of our knowledge, this is the first report on both kinetics of human PNP with MESG and phosphate and crystal structure of PNP from any source in complex with this substrate analogue. It is hoped that the results reported here will aid the rational design of more potent inhibitors of purine nucleoside phosphorylase enzyme activity to be tested as modulators of the immunological system to treat leukemia, autoimmune diseases, and rejection in organ transplantation.

REFERENCES

1. Parks, R. E., Jr., and Agarwal, R. P. (1972) *The enzymes*, Boyer, P. D., Ed., Academic Press, New York, 483-514
2. Kalckar, H. M. (1947) *J. Biol. Chem.* **167,** 429-443
3. Porter, D. J. T. (1992) *J. Biol. Chem.* **267,** 7342-7351
4. Pugmire, M. J., and Ealick, S. E. (2002) *Biochem. J.* **361,** 1-25
5. Giblett, E. R., Ammann, A. J., Wara, D. W., Sandman, R., and Diamond L. K. (1975) *Lancet.* **1,** 1010-1013
6. Stoop, W., Zegers, B. J. M., Hendrickx, G. F. M., van Heukelom, L. H. S., Staal, G. E. J., de Bree, P. K., Wadman, S. K., and Ballieux, R. E. (1977) *N. Engl. J. Med.* **296,** 651-655
7. Stoeckler, J. D. (1984) *Developments in Cancer Chemotherapy*, Glazer, R. I., Ed., CRC Press: Bocca Raton, FL, 35-60
8. Ealick, S. E., Babu, Y. S., Bugg, C. E., Erion, M. D., Guida, W. C., Montgomery, J. A., and Secrist, J. A. (1991) *Proc. Natl. Acad. Sci. USA* **88,** 11540-11544

9. Ealick, S. E., Rule, S. A., Carter D. C., Greenhough, T. J., Babu, Y. S., Cook, W. J., Habash, J., Helliwell, J. R., Stoeckler, J. D., Parks R. E., Jr., Chen, S. F., and Bugg, C. E. (1990) *J. Biol. Chem.* **265,** 1812-1820
10. Kline, P. C., and Schramm, V. L. (1992) *Biochemistry* **31,** 5964-5973
11. Kline, P. C., and Schramm, V. L. (1993) *Biochemistry* **32,** 13212-13219
12. Kline, P. C., and Schramm, V. L. (1995) *Biochemistry* **34,** 1153-1162
13. de Azevedo, W. F., Jr., Canduri, F., dos Santos, D. M., Silva, R. G., Oliveira, J. S., Carvalho, L. P. S., Basso, L. A., Mendes, M. A., Palma, M. S., and Santos, D. S. (2003) *Biochem. Biophys. Res. Commun.* **308,** 545-552
14. de Azevedo, W. F., Jr., Canduri, F., dos Santos, D. M., Pereira J. H., Dias, M. V. B., Silva, R. G., Mendes, M. A., Basso, L. A., Palma, M. S., and Santos, D. S. (2003) *Biochem. Biophys. Res. Commun.* **312,** 767-772
15. Canduri, F., dos Santos, D. M., Silva, R. G., Mendes, M. A., Basso, L. A., Palma, M. S., de Azevedo, W. F., Jr., and Santos, D. S. (2004) *Biochem. Biophys. Res. Commun.* **313,** 907-914
16. Webb, M. R. (1992) *Proc. Natl. Acad. Sci. USA* **89,** 4884-4887
17. Nixon, A. E., Hunter, J. L., Bonifacio, G., Eccleston, J. F., and Webb, M. R. (1998) *Anal. Biochem.* **265,** 299-307
18. Oliveira, J. S., Pinto, C. A., Basso, L. A., and Santos, D. S. (2001) *Protein Express. Purif.* **22,** 430-435
19. Oliveira, J. S, Mendes, M. A., Palma, M. S., Basso, L. A., and Santos, D. S. (2003) *Protein Express. Purif.* **28,** 287-292
20. Silva, R. G., Carvalho, L. P. S., Pinto, C. A., Mendes, M. A., Palma, M. S., Basso, L. A., and Santos, D. S. (2003) *Protein Express. Purif.* **27,** 158-164
21. Collaborative Computer Project Number 4 (1994) *Acta Crystallogr. D.* **50,** 760-763
22. Navaza, J. (1994) *Acta Crystallogr. A.* **50,** 157-163
23. dos Santos, D. M., Canduri, F., Pereira J. H., Dias, M. V. B., Silva, R. G., Mendes, M. A., Palma, M. S., Basso, L. A., de Azevedo, W. F., Jr., and Santos, D. S. (2003) *Biochem. Biophys. Res. Commun.* **308,** 553-559
24. Brünger, A. T. (1992) *X-PLOR Version 3.1: A System for Crystallography and NMR,* Yale University Press, New Haven, CT
25. Laskowski, R. A., MacArthur, M. W., Moss, D. S., and Thornton, J. M. (1993) *J. Appl. Crystllogr.* **26,** 283-291
26. Guex, N., and Peitsch, M. C. (1997) *Electrophoresis* **18,** 2714-2723
27. Cleland, W. W. (1970) *The enzymes*, Boyer, P. D., Ed., Academic Press, New York, 1
28. Segel, I. H. (1975) *Enzyme Kinetics*, John Wiley & Sons, New York, 274-283
29. Basso, L. A., Santos, D. S., Shi, W., Furneaux, R. H., Tyler, P. C., Schramm, V. L., and Blanchard, J. S. (2001) *Biochemistry* **40,** 8196-8203
30. Silva, R. G., Santos, D. S., Basso, L. A., Oses, J. P., Wofchuk, S., Portela, L. W. C., and Souza, D. O. (2004) *Neurochem. Res.* **29,** 1831-1835
31. Erion, M. D., Takabayashi, K., Smith, H. B., Kessi, J., Wagner, S., Hönger, S., Shames, S. L., and Ealick, S. E. (1997) *Biochemistry* **36,** 11725-11734
32. Bzowska, A., Kulikowska, E., and Shugar, D. (1993) *Z. Naturforsch.* **48,** 803-811
33. Bzowska, A. (2002) *Biochim. Biophys. Acta* **1596,** 293-317
34. Bzowska, A., Kulikowska, E., and Shugar, D. (2000) *Pharmacol. Ther.* **88,** 349-425
35. de Azevedo, W. F., Jr., Canduri, F., dos Santos, D. M., Pereira J. H., Dias, M. V. B., Silva, R. G., Mendes, M. A., Basso, L. A., Palma, M. S., and Santos, D. S. (2003) *Biochem. Biophys. Res. Commun.* **309,** 917-922
36. Canduri, F., Fadel, V., Basso, L. A., Dias, M. V. B., Palma, M. S., Santos, D. S., and de Azevedo, W. F., Jr., (2005) *Biochem. Biophys. Res. Commun.* **326,** 335-338
37. Kicska, G. A., Tyler, P. C., Evans, G. B., Furneaux, R. H., Shi, W., Fedorov, A., Lewandowicz, A., Cahill, S. M., Almo, S. C., and Schramm, V. L. (2002) *Biochemistry* **41,** 14489-14498
38. Bzowska, A., Luic, M., Schröder, W., Shugar, D., Saenger, W., Koellner, G. (1995) *FEBS Lett.* **367,** 214-218

39. Koellner, G., Luic, M., Shugar, D., Saenger, W., Bzowska, A. (1997) *J. Mol. Biol.* **265,** 202-216
40. Mao, C., Cook, W. J., Zhou, M., Fedorov, A., Almo, S. C., Ealick, S. E. (1998) *Biochemistry* **37,** 7135-7146
41. Fedorov, A., Shi, W., Kicska, G. A., Fedorov, E., Tyler, P. C., Furneaux, R. H., Hanson, J. C., Gainsford, G. J., Larese, J. Z., Schramm, V. L., and Almo, S. C. (2001) *Biochemistry* **40,** 853-860
42. Shi, W., Basso, L. A., Santos, D. S., Tyler, P. C., Furneaux, R. H., Blanchard, J. S., Almo, S. C., and Schramm, V. L. (2001) *Biochemistry* **40,** 8204-8215
43. Zoltewicz, J. A., Clark, D. F., Sharpless, T. W., and Grabe, G. (1970) *J. Am. Chem. Soc.* **92,** 1741-1750
44. Bzowska, A., Kulikowska, E., Darzynkiewicz, E., and Shugar, D. (1988) *J. Biol. Chem.* **263,** 9212-9217
45. Farutin, V., Masterson, L., Andricopulo, A. D., Cheng, J., Riley, B., Hakimi, R., Frazer, J. W., and Cordes, E. H. (1999) *J. Med. Chem.* **42,** 2422-2431
46. Ropp, P. A., and Traut, T. W. (1991) *J. Biol. Chem.* **266,** 7682-7687
47. Kim, B. K., Cha, S., and Parks, R. E., Jr. (1968) *J. Biol. Chem.* **243,** 1771-1776
48. Cheng, J., Farutin, V., Wu, Z., Jacob-Mosier, G., Riley, B., Hakimi, R., and Cordes, E. H. (1999) *Bioorg. Chem.* **27,** 307-325
49. Erion, M. D., Stoeckler, J. D., Guida, W. C., Walter, R. L., and Ealick, S. E. (1997) *Biochemistry* **36,** 11735, 11748
50. Tebbe, J., Bzowska, A., Wielgus-Kutrowska, B., Schröder, W., Kazimierczuk, Z., Shugar, D., Saenger, W., and Koellner, G. (1999) *J. Mol. Biol.* **294,** 1239-1255
51. Lin, J., and Frey, P. A. (2000) *J. Am. Chem. Soc.* **122,** 11258-11259

FOOTNOTES

* Financial support for this work was provided by Millennium Initiative Program MCT-CNPq, Ministry of Health – Secretary of Health Policy (Brazil) to D.S.S. and L.A.B., and by SMOLBNet, Proc. 01/07532-0, 02/04383-7, 02/00217-0 – FAPESP (São Paulo, Brazil). D.S.S. and L.A.B. also acknowledge grants awarded by CNPq and FINEP. We thank Dr. Osmar Norberto de Souza for assistance with structure analysis, and Dr. John S. Blanchard for his generous gift of MESG.

[1] Abbreviations used: PNP, purine nucleoside phosphorylase; HsPNP, human purine nucleoside phosphorylase; Glu, glutamate; Asn, asparagine; P_i, inorganic phosphate; MESG, 7-methyl-6-thio-guanosine; *V*, maximal velocity; K_m, Michaelis constant; k_{cat}, catalytic constant; Ala, alanine; Ser, serine; Pro, proline; Thr, threonine; Leu, leucine; Phe, phenilalanine; His, histidine; Lys, lysine; Ino, inosine; ddI, 2'-3'-dideoxyinosine; ImmH, immucillin-H; H-bond, hydrogen bond; ImmG, immucillin-G; bPNP, bovine purine nucleoside phosphorylase; Met, methionine; Tyr, tyrosine; K_i, inhibition constant;

[2] PDB accession number 1PWY

[3] PDB accession number 1YRY

[4] PDB accession number 1M73

FIGURE LEGENDS

Fig. 1. Structure of 7-methyl-6-thio-guanosine (MESG), a synthetic substrate of purine nucleoside phohphorylase.

Fig. 2. A, Saturation plots of HsPNP with MESG as the variable substrate. Each curve represents varied-fixed [P_i], ranging from 10 μM – 1600 μM. Initial steady-state rates were obtained by adding enzyme (0.9 ng mL^{-1}) to the reaction mix with several [MESG] (10 μM – 500 μM). B, Double-reciprocal plots obtained from the saturation curves. Inset shows a replot of y-axis intersects against the reciprocal of varied-fixed P_i concentrations. One PNP unity is the amount of enzyme that catalyzes the phosphorolysis of 1 μmol of MESG per min in 1cm optical path.

Fig. 3. A, Saturation plots of HsPNP with P_i as the variable substrate. Each curve represents a varied-fixed [MESG], ranging from 10 μM – 500 μM. Initial steady-state rates were obtained by adding enzyme (0.9 ng mL^{-1}) to the reaction mix with several [P_i] (10 μM – 1600 μM). B, Double-reciprocal plots obtained from the saturation curves. Inset shows a replot of y-axis intersects against the reciprocal of varied-fixed MESG concentrations. One PNP unity is the amount of enzyme that catalyzes the phosphorolysis of 1 μmol of MESG per min in 1cm optical path.

Fig. 4. Ribbon diagrams of HsPNP monomer of apoenzyme (A) and that of the complex with MESG (B). There is an helix-to-coil transition upon binding of MESG, involving residues Ala262-Ala267. The opposite occurs with residues Thr97-Leu105. The region around His257 remains as a coil.

Fig. 5. Ribbon diagrams of HsPNP in complexes with inosine (A), ddI (B), and MESG (C). The side chains of His257 and Asn243 are at longer distances from the ligand in HsPNP:MESG complex as compared to their position in the inosine and ddI structures, whereas Phe200 occupies the same position in all three complexes.

Fig. 6. Stick representation of the active site of HsPNP occupied by MESG and sulfate group. The color scheme is as follows: carbon, gray; oxygen, red; nitrogen, blue; sulfate, yellow. The red sphere is the oxygen atom of a water molecule. Dotted-lines represent hydrogen bonds, except that between a sulfate oxygen and the ring oxygen of ribose, which just shows the distance separating these atoms, and that between Asn243 and N7 of MESG, which represents an ion-dipole electrostatic interaction.

Table I: Kinetic parameters for HsPNP with MESG and P_i

Constant[a]	MESG	P_i	HsPNP
K_m (μM)	358 ± 23	94 ± 10	
V (U mg^{-1})[b]			75 ± 7
k_{cat} (s^{-1})[c]			40 ± 6
Specificity (M^{-1} s^{-1})[d]	1.1 x 10^5	4.3 x 10^6	

[a]Each value is expressed as mean ± sd for two values of the same constant calculated by different plots (see Materials and Methods).

[b]1 unit of HsPNP is defined as the amount of enzyme necessary to convert 1 μmol of MESG in 7-methyl-6-thio-guanine min^{-1} in an optical path of 1 cm.

[c]Catalityc constant, obtained by dividing V per total active site amount.

[d]Specificity constant (k_{cat}/K_m).

Table II: Data collection and refinement statistics

Statistics	HsPNP:MESG
Cell parameters	
$a = b$ (Å)	138.99
c (Å)	159.85
Space group	R32
Number of measurements with I>2σ(I)	92119
Number of independent reflections	14790
Completeness in the range from 56.32 to 2.8 Å (%)	99.9
R_{sym}[a] (%)	8.9
Highest resolution shell (Å)	2.8
Completeness in the highest resolution shell (%)	99.9
R_{sym}[a] in the highest resolution shell (%)	29.9
Resolution range used in the refinement (Å)	7.0 – 2.8
R_{factor}[b] (%)	20.7
R_{free}[c] (%)	29.0
Observed r.m.s.d from ideal geometry	
Bond lenghts (Å)	0.012
Bond angles (°)	1.85
Dihedrals (°)	25.15
B values[d] (Å^2)	
Main chain	37.71
Side chains	39.10
MESG	55.96
Waters	38.33
Sulfate groups	37.36
Residues in the most favored regions of Ramachandran plot (%)	84.0
Residues in additionally allowed regions of Ramachandran plot (%)	13.1
Residues in generously allowed regoins of Ramachandran plot (%)	1.2
Residues in the disallowed regoins of Ramachandran plot (%)	1.6
Number of water molecules	119
Number of sulfate groups	3

[a] $R_{sym} = 100\ \Sigma\ |\ I(h) - \langle I(h)\rangle\ |\ /\ \Sigma\ I(h)$ with $I(h)$, observed intensity and $\langle I(h)\rangle$, mean intensity of reflection h over all measurements of I(h).

[b] $R_{factor} = 100\ \Sigma\ |\ F_{obs} - F_{calc}\ |\ /\ \Sigma\ (F_{obs})$, the sums being taken over all reflections with $F/\sigma\ (F) > 2$ cutoff.

[c] R_{free} = R_{factor} for 10% of the data, which were not included during crystalographic refinement.

[d] B values = average B values for all non-hydrogen atoms.

Structure and kinetics of human PNP complexed with MESG

Fig. 1

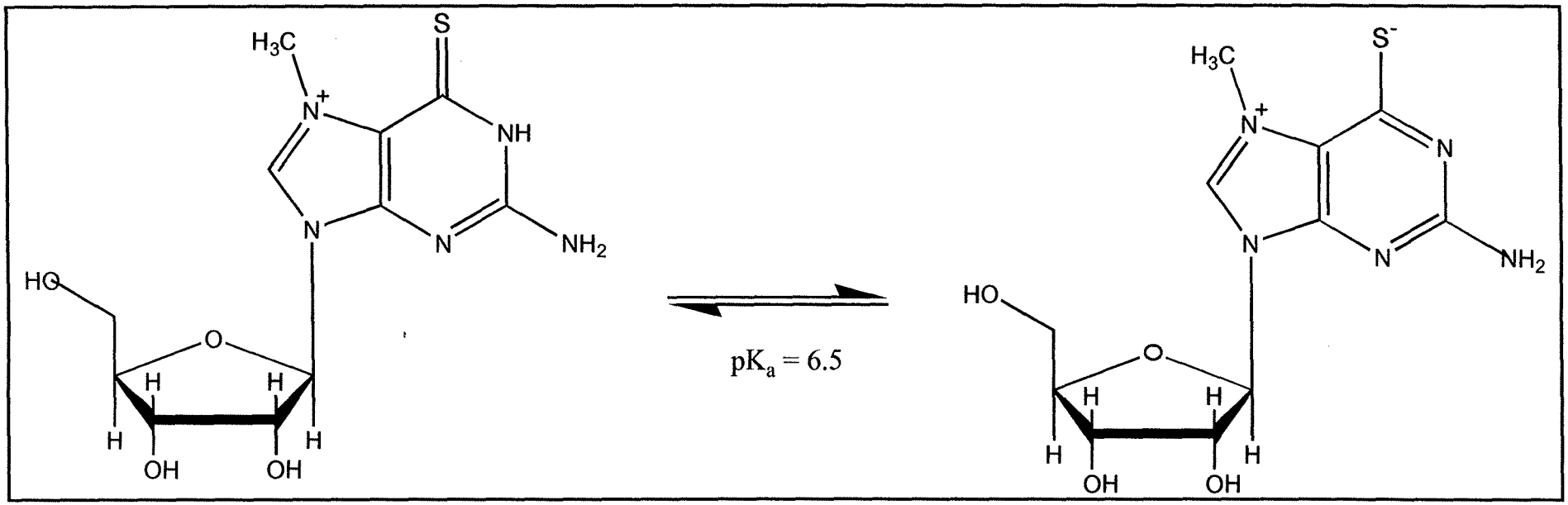

Fig. 2A

Structure and kinetics of human PNP complexed with MESG

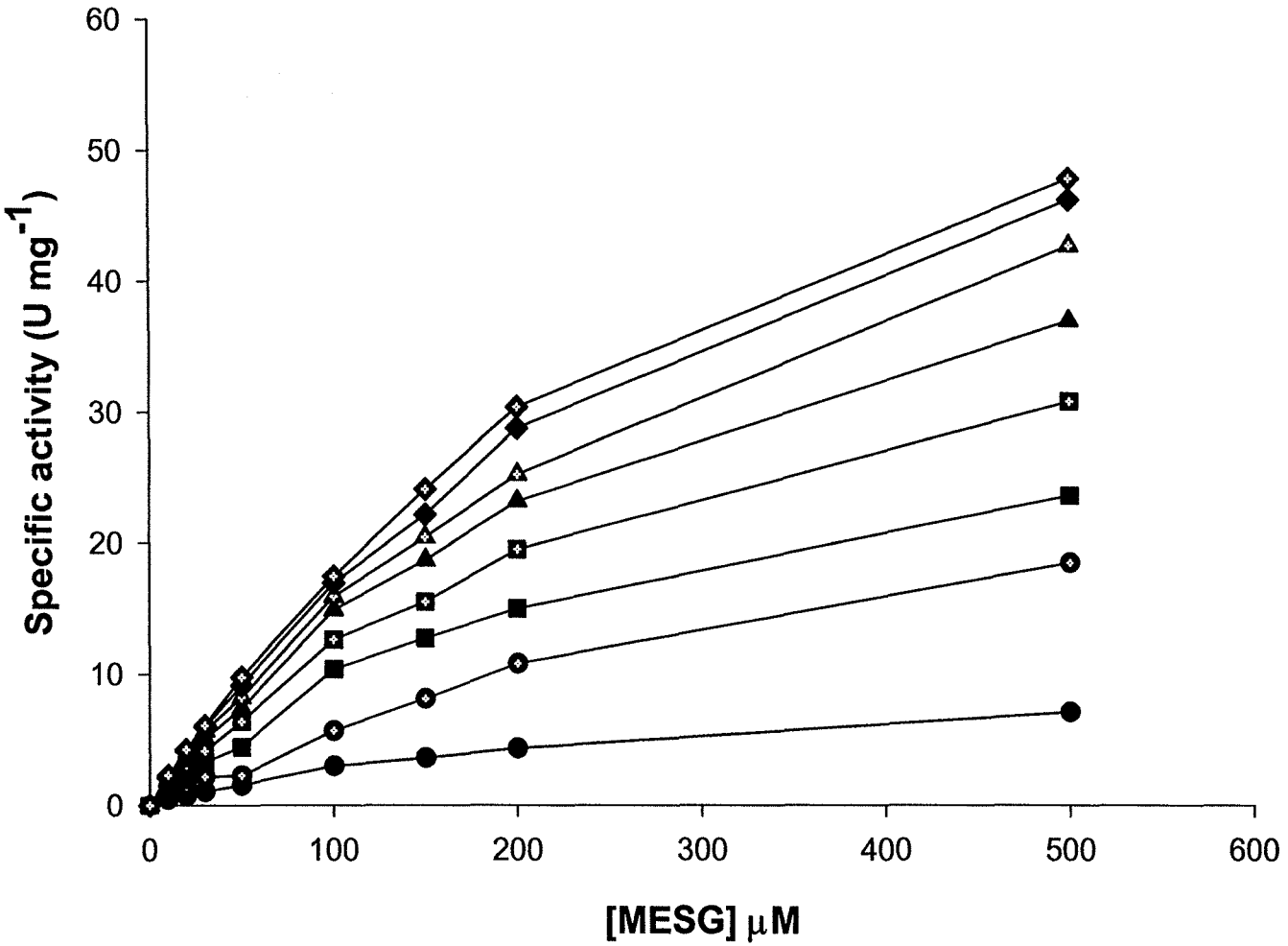

Fig. 2B

Structure and kinetics of human PNP complexed with MESG

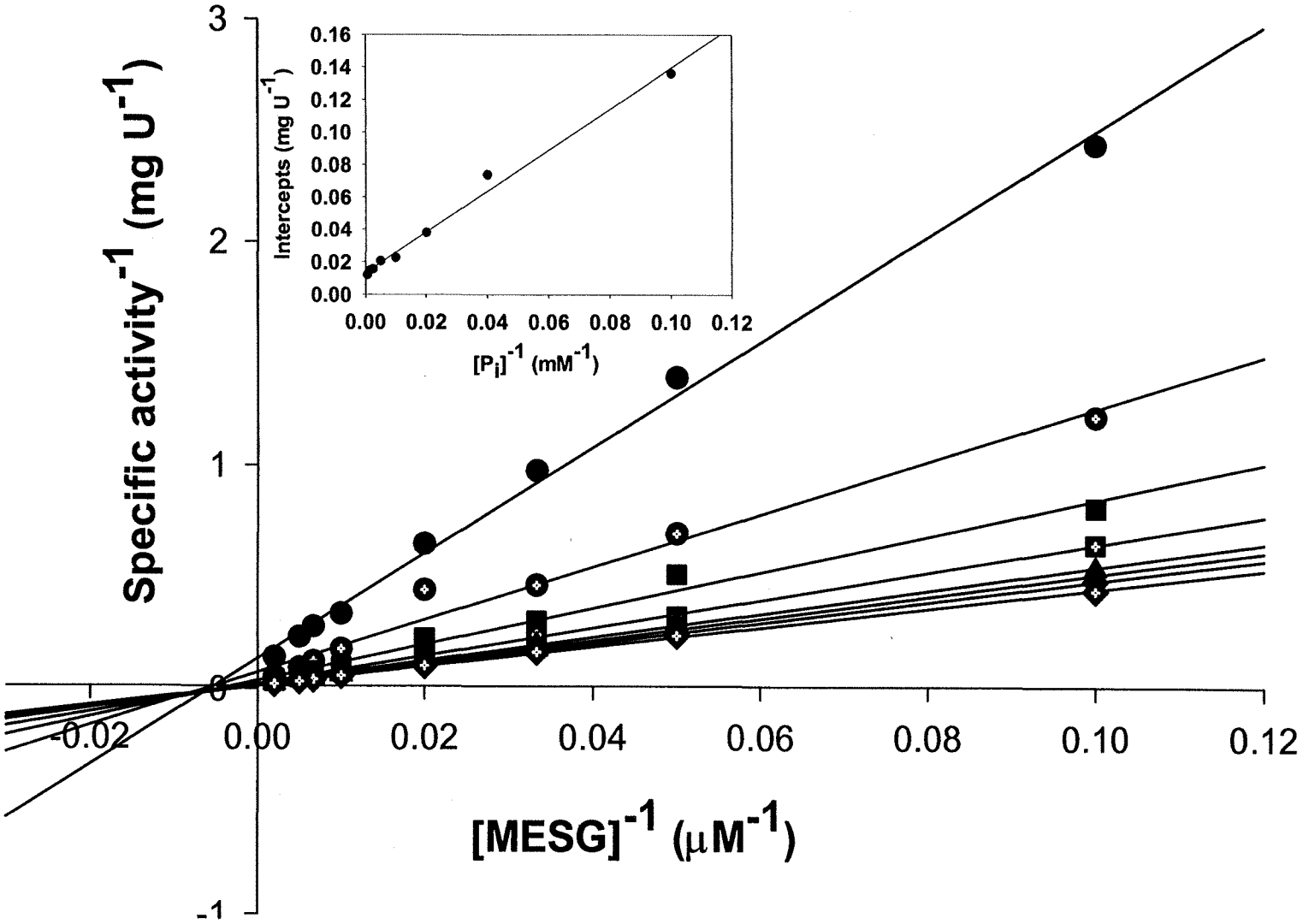

Fig. 3A

Structure and kinetics of human PNP complexed with MESG

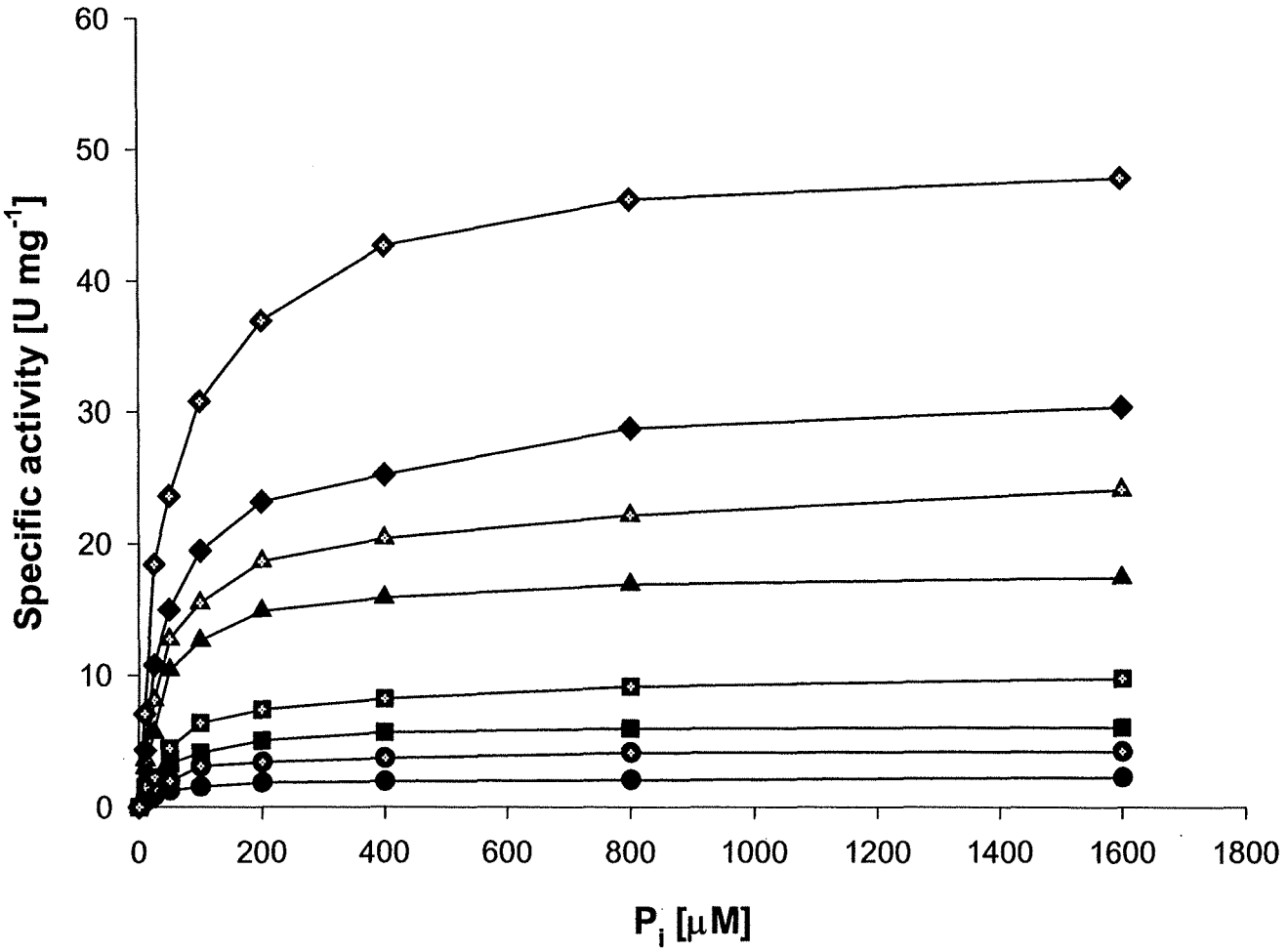

Fig. 3B

Structure and kinetics of human PNP complexed with MESG

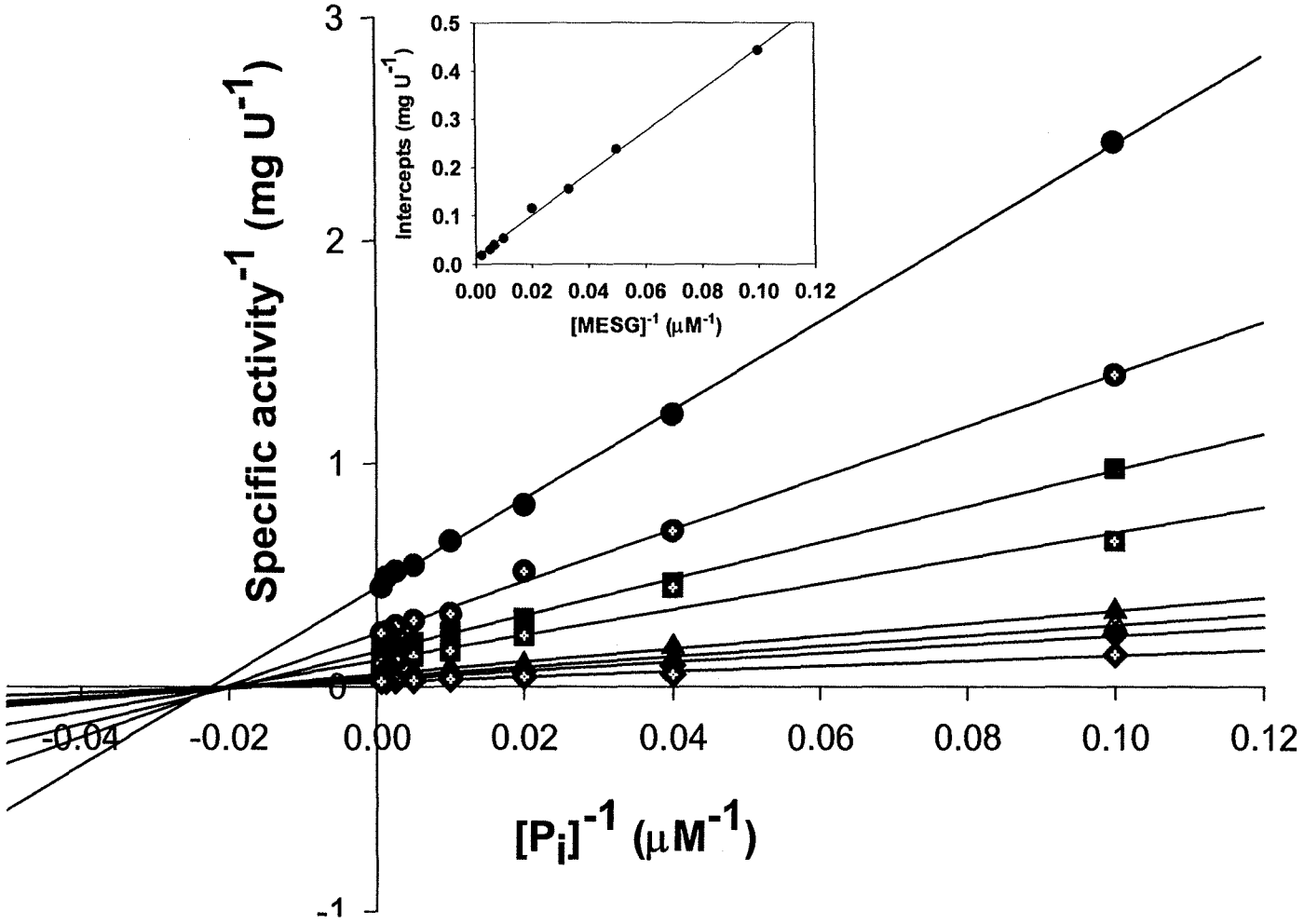

Structure and kinetics of human PNP complexed with MESG

Fig. 4

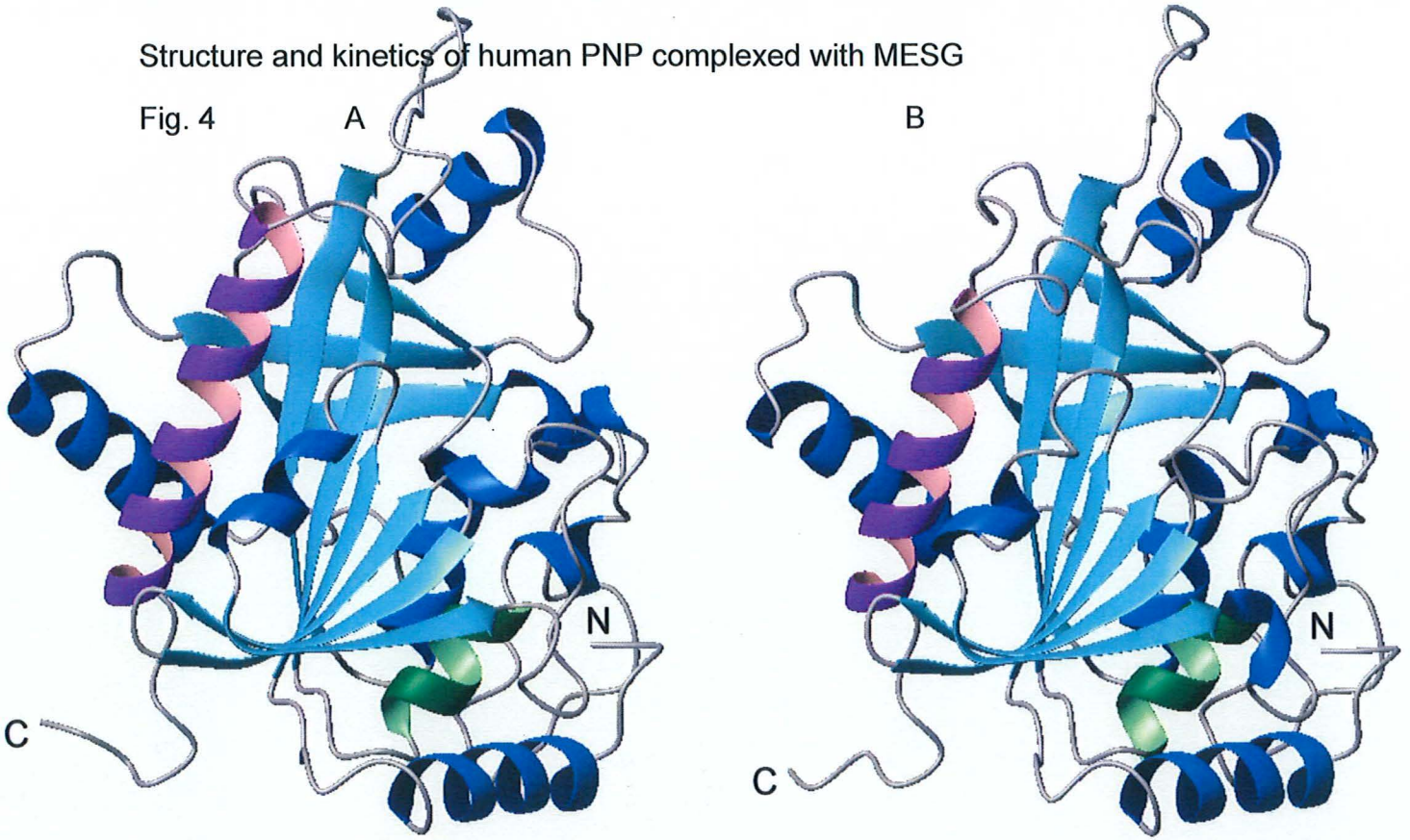

Structure and kinetics of human PNP complexed with MESG

Fig 5A

Structure and kinetics of human PNP complexed with MESG

Fig 5B

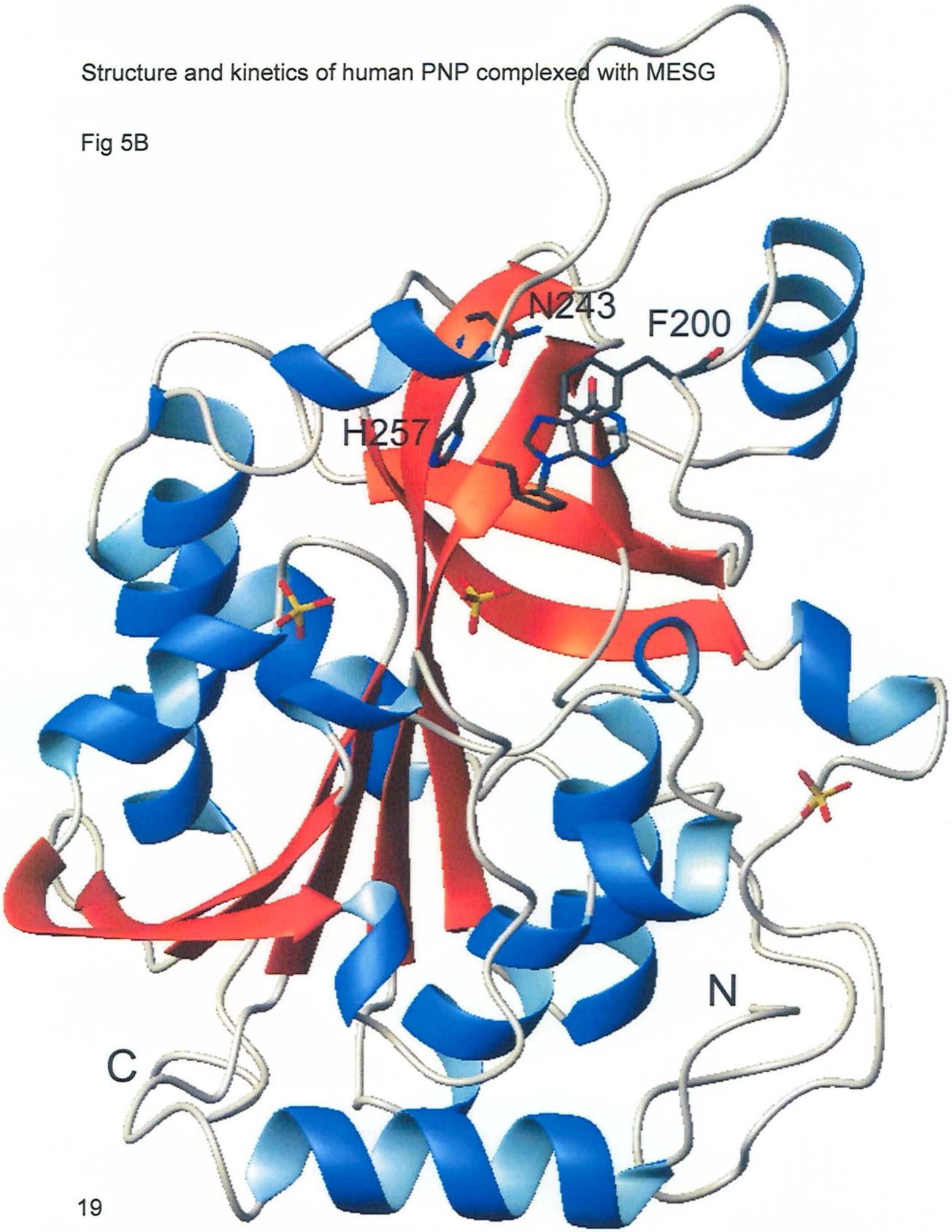

Structure and kinetics of human PNP complexed with MESG

Fig 5C

Structure and kinetics of human PNP complexed with MESG

Fig 6

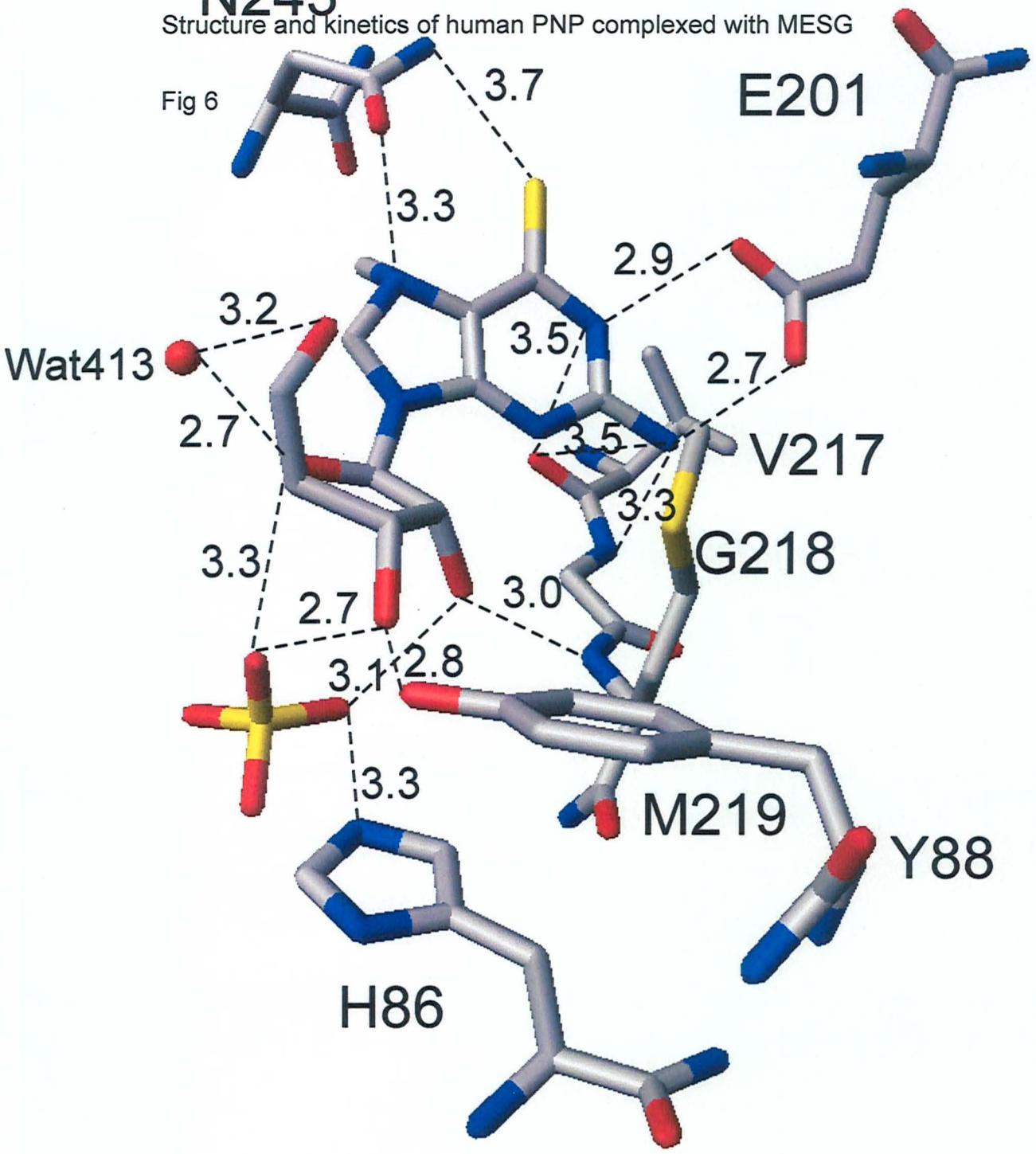

5. Conclusões e perspectivas

Atividade da enzima purino nucleosídeo fosforilase está presente em líquido cérebro espinhal de rato. A diálise das amostras permitiu medir a atividade enzimática sem interferência de compostos tais como nucleosídeos naturais e P_i presentes nesse meio. A atividade da enzima foi completamente abolida pela adição do inibidor imucilina-H, um análogo de estado de transição extremamente específico para PNPs triméricas, confirmando a presença dessa enzima em líquido cérebro espinhal. O valores de K_M aparente para MESG e P_i são, respectivamente, 142 μM e 186 μM, e os valores de V, na mesma ordem, 0,0102 U mg^{-1} e 0,0104 U mg^{-1}. Outros experimentos poderão elucidar um possível papel dessa enzima na proteção neural.

Os experimentos de cinética em estado estacionário indicam uma adição seqüencial dos substratos à PNP humana. Uma constante de especificidade de 1.1×10^5 para MESG demonstra que esse é um substrato mais pobre, quando comparado a inosina, guanosina e análogos alquilados na posição 7. Este resultado pode ser explicado estruturalmente pela perda de uma ligação de hidrogênio entre Asn243 e posição 6 da base nitrogenada, pois tióis formam ligações de hidrogênio muito fracas. A presença de um grupamento metila ligado ao nitrogênio 7 da base não impede a formação de uma interação íon-dipolo entre esse átomo e Asn243. A hidroxila 5' da ribose não está ligada a His257, mas à molécula de água presente no sítio ativo. Estudos cinéticos de inibição por produto, bem como a obtenção da estrutura da PNP com o produto 7-metil-6-tio-guanina poderão auxiliar na elucidação do mecanismo de reação dessa enzima com MESG.

6. Referências

Bantia, S., Ananth, S. L., Parker, C. D., Horn, L., Upshaw, R. (2003) Mechanism of inhibition of T-acute lymphoblastic leukemia cells by PNP inhibitor BCX-1777. *International immunopharmacology* **3,** 879-887.

Barsotti, C., Tozzi, M. G., Ipata, P. L. (2002) Purine and pyrimidine salvage pathway in whole rat brain. *Journal of Biological Chemistry* **277,** 9865-9869.

Basso, L. A., Santos, D. S., Shi, W., Furneaux, R. H., Tyler, P. C., Schramm, V. L., Blanchard, J. S. (2001) Purine nucleoside phosphorylase from *Mycobacterium tuberculosis*. Analysis of inhibition by a trasition-state analogue and dissection by parts. *Biochemistry* **40,** 8196-8203.

Bzowska, A., Luic, M., Schröder, W., Shugar, D., Saenger, W., Koellner, G. (1995) Calf spleen purine nucleoside phosphorylase: purification, sequence and crystal structure of its complex with an *N(7)*-acycloguanosine inhibitor. *FEBS Letters* **367,** 214-218.

Canduri, F., dos Santos, D. M., Silva, R. G., Mendes, M. A., Basso, L. A., Palma, M. S., de Azevedo, W. F., Jr., and Santos, D. S. (2004) Structures of purine nucleoside phosphorylase complexed with inosine and ddI. *Biochemical and Biophysical Research Communication* **313,** 907-914.

Cheng, J., Farutin, V., Wu, Z., Jacob-Mosier, G., Riley, B., Hakimi, R., Cordes, E. H. (1999) Purine nucleoside phosphorylase-catalyzed, phosphate-independent hydrolysis of 2-amino-6-mercapto-7-methylpurine ribonucleoside. *Bioorganic Chemistry* **27,** 307-325.

Cunha, R. A. (2001) Adenosine as a neuromodulator and as a homeostatic regulator in the nervous system: different sources and different receptors. *Neurochemistry International* **38,** 107-125.

de Azevedo, W. F., Jr., Canduri, F., dos Santos, D. M., Silva, R. G., Oliveira, J. S., Carvalho, L. P. S., Basso, L. A., Mendes, M. A., Palma, M. S., Santos, D. S. (2003a) Crystal structure of human nucleoside phosphorylase at 2.3 Å resolution. *Biochemical and Biophysical Research Communication* **308,** 545-552.

de Azevedo, W. F., Jr., Canduri, F., dos Santos, D. M., Pereira J. H., Dias, M. V. B., Silva, R. G., Mendes, M. A., Basso, L. A., Palma, M. S., Santos, D. S. (2003b) Structural basis for inhibition of human PNP by immucillin-H. *Biochemical and Biophysical Research Communication* **309,** 917-922.

de Azevedo, W. F., Jr., dos Santos, G. C., dos Santos, D. M., Olivieri, J. R., Canduri, F., Silva, R. G., Basso, L. A., Renard, G., da Fonseca, I. O., Mendes, M. A., Palma, M. S., Santos, D. S. (2003c) Docking and small angle X-ray scattering studies of purine nucleoside phosphorylase. *Biochemical and Biophysical Research Communication* **309,** 923-928.

dos Santos, D. M., Canduri, F., Pereira J. H., Dias, M. V. B., Silva, R. G., Mendes, M. A., Palma, M. S., Basso, L. A., de Azevedo, W. F., Jr., Santos, D. S. (2003) Crystal structure of purine nucleoside phosphorylase complexed with acyclovir. *Biochemical and Biophysical Research Communication* **308,** 553-559.

Ealick, S. E., Rule, S. A., Carter D. C., Greenhough, T. J., Babu, Y. S., Cook, W. J., Habash, J., Helliwell, J. R., Stoeckler, J. D., Parks R. E., Jr., Chen, S. F., Bugg, C. E. (1990) Three-dimensional structure of human erythrocytic purine nucleoside phosphorylase at 3.2 Å resolution. *Journal of Biological Chemistry* **265,** 1812-1820.

Ealick, S. E., Babu, Y. S., Bugg, C. E., Erion, M. D., Guida, W. C., Montgomery, J. A., Secrist, J. A. (1991) Application of crystallographic and modeling methods in the design of purine nucleoside phosphorylase inhibitors. *Proceedings of National Academy Science USA* **88,** 11540-11544.

Erion, M. D., Takabayashi, K., Smith, H. B., Kessi, J., Wagner, S., Hönger, S., Shames, S. L., Ealick, S. E. (1997) Purine nucleoside phosphorylase. 1. Structure-function studies. *Biochemistry* **36,** 11725-11734.

Farutin, V., Masterson, L., Andricopulo, A. D., Cheng, J., Riley, B., Hakimi, R., Frazer, J. W., and Cordes, E. H. (1999) Structure-activity relationships for a class of inhibitors of purine nucleoside phosphorylase. *Journal of Medicinal Chemistry* **42,** 2422-2431.

Giblett, E. R., Ammann, A. J., Wara, D. W., Sandman, R., Diamond L. K. (1975) Nucleoside phosphorylase deficiency in a child with severe defective T-cell immunity and normal B-cell immunity. *Lancet* **1,** 1010-1013.

Heimer, H. (1999) Outer causes inner conflicts: environment and autoimmunity. *Environment and Health perspectives* **107,** 504-509.

Kalckar, H. M. (1947) Differential spectrophotometry of purine compounds by means of specific enzymes. Determination of hydroxypurine compounds. *Journal of Biological Chemistry.* **167,** 429-443.

Kim, B. K., Cha, S., Parks, R. E., Jr. (1968a) Purine nucleoside phosphorylase from human erythrocytes. I. Purification and properties. *Journal of Biological Chemistry.* **243,** 1763-1770.

Kim, B. K., Cha, S., Parks, R. E., Jr. (1968b) Purine nucleoside phosphorylase from human erythrocytes. II. Kinetic analysis and substrate-binding studies. *Journal of Biological Chemistry.* **243,** 1717-1776.

Kline, P. C., Schramm, V. L. (1992) Purine nucleoside phosphorylase. Inosine hydrolysis, tight binding of the hypoxanthine intermediate, and third-the-sites reactivity. *Biochemistry* **31,** 5964-5973.

Kline, P. C., Schramm, V. L. (1993) Purine nucleoside phosphorylase. Catalytic mechanism and transition-state analysis of the arsenolysis reaction. *Biochemistry* **32,** 13212-13219.

Kline, P. C., Schramm, V. L. (1995) Pre-steady-state transition-state analysis of the hydrolytic reaction catalyzed by purine nucleoside phosphorylase. *Biochemistry* **34,** 1153-1162.

Kicska, G. A., Long, L., Hörig, H., Fairchild, C., Tyler, P. C., Furneaux, R. H., Schramm, V. L., Kaufman, H., L. (2001) Immucillin H, a powerful transition-state analog inhibitor of purine nucleoside phosphorylase, selectively inhibits human T lymphocytes. *Proccedings of National Academy of Science USA* **98,** 4593-4598.

Koellner, G., Luic, M., Shugar, D., Saenger, W., Bzowska, A. (1997) Crystal structure of calf spleen purine nucleoside phosphorylase in a complex with hypoxanthine at 2.15 Å resolution. *Journal of Molecular Biology.* **265,** 202-216.

Lewis, A. S., Glantz, M. D. (1976) Bovine brain purine nucleoside phosphorylase purification, characterization, and catalytic mechanism. *Biochemistry* **15,** 4451-4456.

Litsky, M. L., Charlene, M. H., Lucas, J. H., Jurkowitz, M. S. (1999) Inosine and guanosine preserve neuronal and glial cell viability in mouse spiral cord cultures during chemical hypoxia. *Brain Research* **821,** 426-432.

Mao, C., Cook, W. J., Zhou, M., Fedorov, A., Almo, S. C., Ealick, S. E. (1998) Calf spleen purine nucleoside phosphorylase complexed with substrate and substrate analogues. *Biochemistry* **37,** 7135-7146.

Miles, R. W., Tyler, P. C., Furneaux, R. H., Bagdassarian, C. K., Schramm, V. L. (1998) One-thrid-the-sites transition-state inhibitors for purine nucleoside phosphorylase. *Biochemistry* **37,** 8615-8621.

Nixon, A. E., Hunter, J. L., Bonifacio, G., Eccleston, J. F., and Webb, M. R. (1998) Purine nucleoside phosphorylase: its use in a spectroscopic assay for inorganic phosphate and for removing inorganic phosphate with the aid of phosphodeoxyribomutase. *Analytical Biochemistry* **265,** 299-307.

Oliveira, J. S, Mendes, M. A., Palma, M. S., Basso, L. A., Santos, D. S. (2003) One-step purification of 5-enolpyruvylshikimate-3-phosphate synthase from *Mycobacterium tuberculosis. Protein Expression and Purification* **28,** 287-292.

Parks, R. E., Jr., and Agarwal, R. P. (1972) Purine nucleoside phosphorylase. *The enzymes* **7,** Boyer, P. D., Ed., Academic Press, New York, 483-514.

Parkinson, F. E., Sinclair, C. J. D., Othman, T., Haughey, N. J., Geiger, J. D. (2002) Differences between rat primary cortical neurons and astrocytes in purine release evoked by ischemic conditions. *Neuropharmacology* **43,** 836-846.

Portela, L. W. C., Oses, J. P., Silveira, A. L., Shmidt, A. P., Lara, D. R., Battastini, A. M. O., Ramirez, G., Vinadé, L., Sarkis, J. J. F., Souza, D. O. (2002) Guanine and adenine nucleotidase activities in rat cerebrospinal fluid. *Brain Research* **950,** 74-78.

Porter, D. J. T. (1992) Purine nucleoside phosphorylase. Kinetic mechanism of the enzyme from calf spleen. *Journal of Biological Chemistry.* **267,** 7342-7351.

Pugmire, M. J., Ealick, S. E. (2002) Structural analysis reveal two distinct families of nucleoside phosphorylase. *Biochemical Journal* **361,** 1-25.

Ralevic, V., Burnstock, G. (1998) Receptors for purines and pyrimidines. *Pharmacology Review* **50,** 413-492.

Ries, A. G., Eisner, M. P., Kosary, C. L., Honkey, B. F., Miller, B. A., Cleg, L., Mariotto, A., Fewer, E. J., Edwards, B. K. (2004) SEER Cancer statistics Review 1975-2001. National Cancer Institute, Bethesda, MD.

Roesler, R., Vianna, M. R., Lara, D. R., Izquierdo, I., Schimidt, A. P., Souza, D. O. (2000) Guanosine impairs inhibitory avoidance performance in rats. *Neuroreport* **11,** 2537-2540.

Shi, M., You, S. W., Meng, J. H., Ju, G. (2002) Direct protection of inosine on PC12 cells against zinc-induced injury. *Neuroreport* **13,** 477-479.

Shi, W., Basso, L. A., Santos, D. S., Tyler, P. C., Furneaux, R. H., Blanchard, J. S., Almo, S. C., Schramm, V. L. (2001) Structures of purine nucleoside phosphorylase from *Mycobacterium tuberculosis* in complexes with immucillin-H and its pieces. *Biochemistry* **40,** 8204-8215.

Silva, R. G., Carvalho, L. P. S., Pinto, C. A., Mendes, M. A., Palma, M. S., Basso, L. A., and Santos, D. S. (2003) Cloning, overexpression, and purification of a functional human purine nucleoside phosphorylase. *Protein Expression and Purification* **27,** 158-164.

Stoeckler, J. D., Cambor, C., Parks, R. E., Jr. (1980) Human erythrocyte purine nucleoside phosphorylase: reaction with sugar-modified nucleoside substrates. *Biochemistry* **19,** 102-107.

Stoeckler, J. D. (1984) *Developments in Cancer Chemotherapy*, Glazer, R. I., Ed., CRC Press: Bocca Raton, FL, 35-60.

Stoop, W., Zegers, B. J. M., Hendrickx, G. F. M., van Heukelom, L. H. S., Staal, G. E. J., de Bree, P. K., Wadman, S. K., Ballieux, R. E. (1977) Purine nucleoside phosphorylase deficiency associated with selective cellular immunodeficiency. *New England Journal of Medicine* **296,** 651-655.

Tebbe, J., Bzowska, A., Wielgus-Kutrowska, B., Schröder, W., Kazimierczuk, Z., Shugar, D., Saenger, W., Koellner, G. (1999) Crystal structure of the purine nucleoside phosphorylase (PNP) from *Cellulomonas sp.* and its implication for the mechanism of trimeric PNPs *Journal of Molecular Biology* **294,** 1239-1255.

Webb, M. R. (1992) A continuous spectrophotometric assay for inorganic phosphate and measuring phosphate release kinetics in biological systems. *Proceedings of National Academy of Science USA* **89,** 4884-4887.

Wang, Z. X., Cheng, Q., Killilea, S. D. (1995) A continuous spectrophotometric assay for phosphorylase kinase. *Analytical Biochemistry* **230,** 55-61.

Zimmerman, T. P., Gersten, N. B., Ross, A. F., Miech, R. P. (1971) Adenine as substrate for purine nucleoside phosphorylase. *Canadian Journal of Biochemistry* **49,** 1050-1054.

Anexo: Cloning, overexpression, and purification of functional human purine nucleoside phosphorylase

Publicado na *Protein Expression and Purificat*ion em 2003

ACADEMIC PRESS

Available online at www.sciencedirect.com

SCIENCE DIRECT®

Protein Expression and Purification 27 (2003) 158–164

Protein Expression & Purification

www.elsevier.com/locate/yprep

Cloning, overexpression, and purification of functional human purine nucleoside phosphorylase

Rafael G. Silva,[a] Luiz Pedro S. Carvalho,[a] Jaim S. Oliveira,[a] Clotilde A. Pinto,[a] Maria A. Mendes,[b] Mário S. Palma,[b] Luiz A. Basso,[a,1] and Diógenes S. Santos[a,*]

[a] *Grupo de Microbiologia Molecular e Funcional, Departamento de Biologia Molecular e Biotecnologia, Instituto de Biociências, Universidade Federal do Rio Grande do Sul, Avenida Bento Gonçalves, 9500, Porto Alegre-RS 91501-970, Brazil*

[b] *Laboratório de Biologia Estrutural e Zooquímica (CEIS), Departamento de Biologia, Instituto de Biociências, Universidade do Estado de São Paulo, Rio Claro, SP 13506-900, Brazil*

Received 26 June 2002, and in revised form 5 September 2002

Abstract

Purine nucleoside phosphorylase (PNP) catalyzes the phosphorolysis of the *N*-ribosidic bonds of purine nucleosides and deoxynucleosides. A genetic deficiency due to mutations in the gene encoding for human PNP causes T-cell deficiency as the major physiological defect. Inappropriate activation of T-cells has been implicated in several clinically relevant human conditions such as transplant tissue rejection, psoriasis, rheumatoid arthritis, lupus, and T-cell lymphomas. Human PNP is therefore a target for inhibitor development aiming at T-cell immune response modulation. In addition, bacterial PNP has been used as reactant in a fast and sensitive spectrophotometric method that allows both quantitation of inorganic phosphate (P_i) and continuous assay of reactions that generate P_i such as those catalyzed by ATPases and GTPases. Human PNP may therefore be an important biotechnological tool for P_i detection. However, low expression of human PNP in bacterial hosts, protein purification protocols involving many steps, and low protein yields represent technical obstacles to be overcome if human PNP is to be used in either high-throughput drug screening or as a reagent in an affordable P_i detection method. Here, we describe PCR amplification of human PNP from a liver cDNA library, cloning, expression in *Escherichia coli* host, purification, and activity measurement of homogeneous enzyme. Human PNP represented approximately 42% of total soluble cell proteins with no induction being necessary to express the target protein. Enzyme activity measurements demonstrated a 707-fold increase in specific activity of cloned human PNP as compared to control. Purification of cloned human PNP was achieved by a two-step purification protocol, yielding 48 mg homogeneous enzyme from 1 L cell culture, with a specific activity value of 80 U mg^{-1}.

Purine nucleoside phosphorylase (PNP)[2] catalyzes the reversible phosphorolysis of *N*-ribosidic bonds of both purine nucleosides and deoxynucleosides, except adenosine, generating purine base and ribose (or deoxyribose) 1-phosphate [1]. The major physiological substrates for mammalian PNP are inosine, guanosine, and 2′-deoxyguanosine [2]. PNP is specific for purine nucleosides in the β-configuration and exhibits a preference for ribosyl-containing nucleosides relative to the analogs containing the arabinose, xylose, and lyxose stereoisomers [3]. Moreover, PNP cleaves glycosidic bond with inversion of configuration to produce α-ribose 1-phosphate, as shown by its catalytic mechanism [4]. The human erythrocyte enzyme is active as a trimer, with each subunit presenting a molecular weight of 32,000 [5].

It has been reported that genetic deficiencies of PNP cause gradual decrease in T-cell immunity, though keeping B-cell immunity normal as well as other tissues [6]. The absence of PNP activity is thought to lead to accumulation of deoxyguanosine triphosphate, which inhibits the enzyme ribonucleotide reductase and ensuing DNA synthesis inhibition, thereby preventing cellular proliferation required for an immune response [7].

* Corresponding author. Fax: +55-51-3316-6234.

E-mail addresses: labasso@dna.cbiot.ufrgs.br (L.A. Basso), diogenes@dna.cbiot.ufrgs.br (D.S. Santos).

[1] Also corresponding author.

[2] *Abbreviations used:* ESI-MS, electrospray ionization mass spectrometry; IPTG, isopropyl β-D-thiogalactoside; LB, Luria–Bertani; MESG, 2-amino-6-mercapto-7-methylpurine ribonucleoside; P_i, inorganic phosphate; PNP, purine nucleoside phosphorylase.

1046-5928/02/$ - see front matter © 2002 Elsevier Science (USA). All rights reserved.
PII: S1046-5928(02)00602-2

Thus, this enzyme is a potential target for drug development, which could induce immune suppression to treat, for instance, autoimmune diseases, T cell leukemia, and lymphoma and organ transplantation rejection [8]. Moreover, some PNP inhibitors have been tested in combination with nucleoside antiviral and anticancer drugs, showing the ability to potentiate the in vivo activity of these drugs [9].

In addition, a simple and rapid spectrophotometric method using 2-amino-6-mercapto-7-methylpurine ribonucleoside (MESG) and bacterial PNP has been developed to both quantitate P_i in solutions and to follow kinetics of P_i release from enzymatic reactions [10]. Although the reaction equilibrium favors the nucleoside formation with natural substrates, this synthetic substrate favors the cleavage of its own glycosidic bond [11]. Further studies have shown the possibility of using PNP as coupled enzyme in a continuous spectrophotometric assay for phosphorylase kinase [12] and protein phosphatase catalyzed reactions [13], as well as in combination with phosphodeoxyribomutase to remove P_i from solutions [14].

To pave the way for both using immobilized human PNP enzyme as a target for drug development in high-throughput drug screening and to test its viability as a tool for coupled enzymatic assay, the human PNP encoding cDNA was PCR amplified, cloned, and sequenced. The enzyme was overexpressed in soluble form in *Escherichia coli* BL21(DE3) host cells by a low-cost and simple protocol. The enzyme was purified by a two-step purification protocol, yielding cloned human PNP enzyme with the same specific activity found by other authors. This improved and simpler protocol for human PNP protein production in large quantities will contribute to current efforts towards the search for new drugs and the development of a low-cost P_i detection coupled assay.

Materials and methods

PCR amplification and cloning of human pnp cDNA

Synthetic oligonucleotide primers (First: 5′ a*atg*gaacggatacacctatg 3′, second: 5′ a*tca*actggctttgtcagggag 3′, third: 5′ **tcatatg**gagaacggatacacc 3′, and fourth: 5′ **taagctt***tca* actggctttgtcag 3′) were designed based on the *pnp* cDNA sequence reported [15]. The first and third primers were complementary to the amino-terminal coding strand, and the second and fourth ones, to the carboxyl-terminal coding strand. The start and stop codons are shown in italics. The 5′ *Nde*I and 3′ *Hin*dIII restriction sites of the third and fourth primers are shown in bold. The first and second primers were designed to be complementary to 22 and 21 bases of, respectively, the N- and C-terminal ends of the PNP cDNA. A non-complementary A residue (deoxyadenyl-3′) at the 5′ end of each primer was added to protect the start and stop codons of primers 1 and 2, respectively, since, in our hands, occasionally a base is removed from the 5′-end of primers during PCR amplification experiments (data not shown). Removal of a nucleotide from the 3′-end of the amplification primers would have no effect on the gene product. Moreover, the extra four bases at the 3′-end of primers 1 and 2 were added to improve the likelihood of PCR amplification of the PNP cDNA. The primers (first and second) were used to amplify the *pnp* cDNA (870 bp) from a human liver cDNA expanded library in λ TriplEX phage (Clontec), using standard PCR conditions with a hot start at 99 °C for 10 min, and *Pfu* DNA polymerase (Stratagene). This PCR fragment was cloned into pCR-Blunt vector (Invitrogen) to be employed as DNA template for further amplification attempts. To introduce the 5′ *Nde*I and 3′ *Hin*dIII restriction sites, the third and fourth primers were used to amplify, using the same PCR conditions, the PNP cDNA that was cloned into the pCR-Blunt vector in the first round of PCR amplification. The PCR product was purified by electrophoresis on low-melting agarose, cloned into pCR-Blunt vector, digested with *Nde*I and *Hin*dIII, and ligated into a pET-23a(+) expression vector (Novagen), which had previously been digested with the same restiction enzymes. The DNA sequence of the amplified human *pnp* cDNA was determined using the MegaBace system (Amershan Pharmacia Biotech) to confirm the identity of the cloned DNA and to ensure that no mutations were introduced by the PCR amplification step.

Overexpression of recombinant human PNP

The pET23a(+)::*pnp* recombinant plasmid was transformed into electrocompetent *E. coli* BL21(DE3) cells and selected on LB agar plates containing 50 μg ml^{-1} carbenicillin. Control experiments were performed under the same experimental conditions, except that transformed *E. coli* cells harbored the expression vector lacking the target DNA insert. Single recombinant colonies were used to inoculate 5 ml LB medium containing carbenicillin (50 μg ml^{-1}). To evaluate human PNP protein expression as a function of cell growth phase, *E. coli* BL21(DE3) cells harboring pET-23a(+)::*pnp* recombinant plasmid were grown in the absence of IPTG and samples were removed at various times for OD_{600} measurements and for electrophoretic analysis. The cells were thus incubated at 180 rpm at 37 °C for 5 h10 min, 5 h40 min, 6 h20 min, 9 h20 min, 12 h20 min, and 28 h without addition of IPTG, harvested by centrifugation at 20,800*g* for 20 min, and stored at −20 °C. The stored cells were suspended in 50 mM Tris–HCl (pH 7.6), disrupted by sonication using two 10-s pulses to release the proteins, and cell debris

was separated by centrifugation at 23,500*g* for 30 min at 4 °C. The soluble protein content was analyzed by SDS–PAGE [16]. The proportion of recombinant human PNP to total soluble proteins in SDS–PAGE gels was estimated using a GS-700 imaging densitometer (Bio-Rad).

Purification of recombinant human PNP

Single colonies *E. coli* BL21(DE3) harboring the recombinant plasmid were used to inoculate 1 L LB medium containing 50 μg ml^{-1} carbenicillin and grown for 22 h at 37 °C and 180 rpm for large scale protein production. Cells (4 g) were harvested by centrifugation at 20,800*g* at 4 °C and stored at −20 °C. The cells were suspended in 15 ml of 50 mM Tris–HCl (pH 7.6) (buffer A), incubated for 30 min in the presence of lysozyme (0.2 mg ml^{-1}), disrupted by sonication as described above, and centrifuged at 48,000*g* for 60 min at 4 °C. The supernatant was incubated with 1% (w/v) of streptomycin sulfate and centrifuged at 48,000*g* for 30 min at 4 °C. The supernatant was dialyzed against buffer A and centrifuged at 48,000*g* for 30 min at 4 °C. The resulting supernatant was loaded on an FPLC Q-Sepharose Fast Flow (26 × 9.5) column (Amershan Pharmacia Biotech) pre-equilibrated with the same buffer. The column was washed with 10 volumes of the same buffer and the absorbed material was eluted with a linear gradient (0–100%) of 20 times the column volume of 50 mM Tris–HCl, 0.2 mM NaCl (pH 7.6) (buffer B). The recombinant protein eluted from the anion exchange column at 40% buffer B, the fractions were pooled (82 ml), concentrated down to 6.6 ml using an Amicon ultrafiltration cell (MWCO 10,000 Da), and applied to an FPLC Sephacryl S-200 (26 × 60) (Amersham Pharmacia Biotech) column pre-equilibrated with buffer A. The column was run with 1 volume of the same buffer. The recombinant human PNP protein eluted in a total volume of 10 ml and stored in 85% ammonium sulfate solution. The protein content was analyzed by SDS–PAGE [16].

Protein determination

Protein concentration was determined by the method of Bradford et al. [17] using the Bio-Rad protein assay kit (Bio-Rad) and bovine serum albumin as standard.

Mass spectrometry analyses

The homogeneity of protein preparation was assessed by mass spectrometry (MS), employing some adaptations made to the system described by Chassaigne and Lobinski [18]. Samples were analyzed on a triple quadrupole mass spectrometer, model QUATTRO II, equipped with a standard electrospray (ESI) probe (Micromass, Altrinchan), adjusted to ca. 250 μl min^{-1}. The source temperature (80 °C) and needle voltage (3.6 kV) were maintained constant throughout the experimental data collection, applying a drying gas flow (nitrogen) of 200 L h^{-1} and a nebulizer gas flow of 20 L h^{-1}. The mass spectrometer was calibrated with intact horse heart myoglobin and its typical cone-voltage induced fragments. The subunit molecular mass of recombinant human PNP was determined by ESI-MS, adjusting the mass spectrometer to give a peak width at half-height of 1 mass unit, and the cone sample to skimmer lens voltage controlling the ion transfer to mass analyzer was set to 38 V. About 50 pmol (10 μl) of each sample was injected into electrospray transport solvent. The ESI spectrum was obtained in the multi-channel acquisition mode, scanning from 500 to 800 m/z at scan time of 5 s. The mass spectrometer is equipped with MassLynx and Transform softwares for data acquisition and spectra handling.

N-terminal amino acid sequencing

The N-terminal amino acid residues of purified recombinant human PNP were identified by automated Edman degradation sequencing using a PPSQ 21A gas-phase sequencer (Shimadzu).

Purine nucleoside phosphorylase assay

Recombinant human PNP was assayed in the forward direction in 50 mM Tris–HCl, pH 7.6. Enzyme activity was measured by the difference in absorbance between 2-amino-6-mercapto-7-methylpurine ribonucleoside (MESG) and the purine base product of its reaction with inorganic phosphate (P_i) catalyzed by PNP [10]. The bacterial PNP enzyme and MESG are commercially available as the Enzchek phosphate assay kit (Molecular Probes); the assay was performed by replacing the commercial PNP by the recombinant human PNP. This reaction gives an absorbance increase at 360 nm with an extinction coefficient value of 11,000 M^{-1} cm^{-1} at pH 7.6 [10]. Initial steady-state rates were calculated from the linear portion of the reaction curve for extracts of *E. coli* BL21(DE3) cells harboring pET-23a(+)::*pnp* plasmid and all fractions of the purification protocol.

Results and discussion

The nucleotide sequence analysis using the dideoxy-chain termination method of the PCR-amplified human *pnp* cDNA (870 bp) confirmed the identity of the coding DNA sequence of cloned fragment and demonstrated that no mutations were introduced by the PCR amplification steps. Although the strategy used here for cloning did not involve complementation [19] and

hybridization [15] previously used for cloning *pnp* cDNA, it proved to be suitable and efficient. Probably, owing to the lack of complete sequence complementarity between primers three and four and cDNA, no PCR product of the correct size (870 bp) could be obtained using these restriction site-containing primers under a number of experimental conditions tested for amplification. Hence, the *pnp* cDNA was first cloned without restriction sites and re-amplified from this recombinant plasmid using the restriction site-containing primers (third and fourth ones).

Human PNP was overexpressed in *E. coli* BL21(DE3) cells carrying pET-23a(+)::*pnp* recombinant plasmids. Analysis by SDS–PAGE with Coomassie blue staining indicated that the cell extracts contained a significant amount of protein with subunit molecular weight in agreement with the expected MW for human PNP [5] (Fig. 1). Densitometric quantification of the SDS–PAGE protein bands showed that recombinant human PNP constituted approximately 42% of total protein present in the soluble cell extract under the experimental conditions used. Enzyme activity measurements demonstrated that there was a 707-fold increase in specific activity for human PNP when *E. coli* harboring either pET-23a(+)::*pnp* or pET-23a(+) crude extracts were compared (Table 1). Contrary to what was previously described for this enzyme [20], where human PNP represented about 5% of total protein present in the soluble cell extracts with addition of IPTG (1 mM final concentration), overexpression was achieved here (after 22 h of cell growth) with no addition of IPTG.

Recombinant human PNP protein expression as a function of cell growth phase in the absence of IPTG could be detected at all time intervals tested (Fig. 2). However, recombinant human PNP protein expression

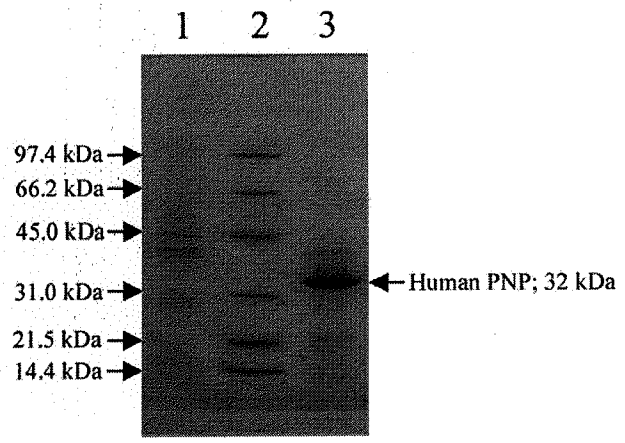

Fig. 1. SDS–PAGE analysis of protein-soluble crude extracts. Overexpression of human PNP after 22 h of cell growth in LB medium without addition of IPTG. Lane 1, *E. coli* BL21(DE3) [pET-23a(+)] (control); lane 2, MW markers; lane 3, *E. coli* BL21(DE3) [pET-23a(+)::*pnp*].

Table 1
Measurements of recombinant human purine nucleoside phosphorylase enzyme activity

Cell extract[a]	Sp act[b] (SA, $U mg^{-1}$)	SA cloned/SA control
Control	0.02	1.00
PNP	17.04	707.10

[a] Cell crude extract in 50 mM Tris–HCl, pH 7.6.
[b] $U ml^{-1}/mg ml^{-1}$.

in *E. coli* BL21(DE3) host cells as compared to the control cells transformed with pET-23a(+) plasmid appeared to reach a maximum in the stationary phase (Fig. 2). The values for the proportion of recombinant human PNP to total soluble protein indicated in Fig. 2 are underestimates, since lower loads of protein on SDS–PAGE indicated a proportion of approximately 40% human PNP to total soluble protein after 22 h of growth (data not shown), in agreement with the results presented in Fig. 1.

Hosts for pET vectors (Novagen) harbor the highly processive T7 RNA polymerase under control of the IPTG-inducible *lac*UV5 promoter. Although it is often argued that the cost of IPTG limits the usefulness of *lac* promoter to high-added-value products, it was shown here that high levels of expression of human PNP could be obtained with pET vectors as cells entered the stationary phase without addition of inducer in LB medium. Similar experimental observations were reported using the pET system [21,22]. It has been demonstrated that when λDE3 hosts are grown to stationary phase in media lacking glucose, cyclic AMP mediated derepression of both the wild type and *lacUV5* promoters occurs [23]. These authors also proposed that cyclic AMP, acetate, and low pH are required to high-level expression in the absence of IPTG induction when cells approach stationary phase in complex medium, and that derepression of the *lac* operon in the absence of IPTG may be part of a general cellular response to nutrient limitation. As described in the pET System Manual (www.novagen.com), the *E. coli* BL21(DE3) host strain is a lysogen of bacteriophage DE3, a lambda derivative that carries a DNA fragment containing the *lacI* gene, the *lacUV5* promoter, and the gene for T7 RNA polymerase. This fragment is inserted into the *int* gene, preventing DE3 from integrating into or excising from the chromosome without a helper phage. Once a DE3 lysogen is formed, the only promoter known to direct transcription of the T7 RNA polymerase gene is the *lacUV5* promoter, which is inducible by IPTG. A characteristic of the pET-23a(+) expression vector is that it contains a "plain" T7 promoter. Background expression is minimal in the absence of T7 RNA polymerase because the host RNA polymerases do not initiate from T7 promoters and the cloning sites in pET plasmids are in regions weakly transcribed (if at all) by

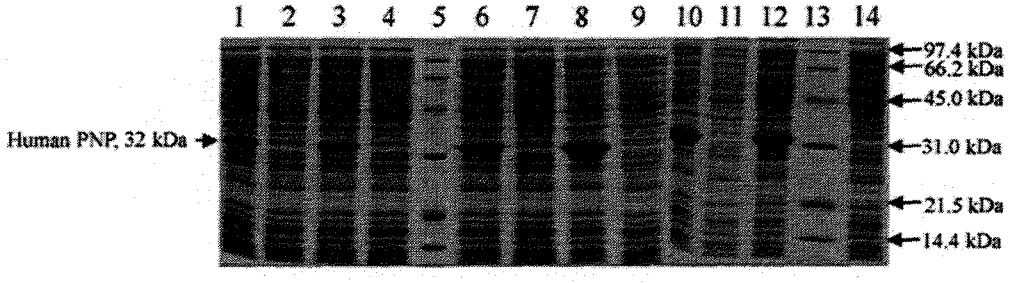

Fig. 2. SDS–PAGE analysis of total soluble protein as a function of growth time. A time course showing an increase of recombinant human PNP expression in the stationary phase. Lanes 5 and 13, MW markers; lanes 2, 4, 7, 9, 11, and 14, *E. coli* BL21(DE3) [pET-23a(+)] (control); lanes 1, 3, 6, 8, 10, and 12, *E. coli* BL21(DE3) [pET-23a(+)::*pnp*]. In brackets are given the values for, respectively, time intervals of sample removal, their OD_{600}, human PNP proportion to total soluble protein for the following lanes: 1 (5 h10 min, 0.315, 9.7%), 3 (5 h40 min, 0.380, 10.8%), 6 (6 h20 min, 0.511, 13.9%), 8 (9 h20 min, 0.846, 21.7%), 10 (12 h20 min, 1.440, 31.6%), and 12 (28 h, 4.358, 30.0%).

read-through activity of bacterial RNA polymerase. The fragment of DNA cloned into the pET-23a(+) vector harbors no other piece of DNA, except the coding DNA sequence of human PNP. It seems therefore unlikely that other promoter is present that might titrate out the *lac* repressor.

Human PNP was purified as described in Materials and methods and analyzed by SDS–PAGE with Coomassie blue staining. The relative mobility of the polypeptide chain in SDS–PAGE indicates a homogeneous protein with molecular weight value of approximately 32 kDa (Fig. 3). The enzymatic assay and protein concentration determination showed a specific activity of $80 \pm 3\,U\,mg^{-1}$ for the homogeneous target protein with MESG as substrate, indicating that the protein purification protocol used resulted in a 3.2-fold purification (Table 2). The specific activity value for the recombinant human PNP compares favorably with the value of $55\,U\,mg^{-1}$ for the homogeneous human erythrocyte PNP using guanosine as substrate [5]. Approximately 48 mg of homogeneous cloned human PNP protein could be obtained from 4 g of cells or, stated otherwise, approximately $48\,mg\,L^{-1}$ of LB medium (Table 2). Protocols for human PNP purification have been described either using erythrocytes [1,5,24] or prokaryotic host cells expressing recombinant human PNP [20,25].

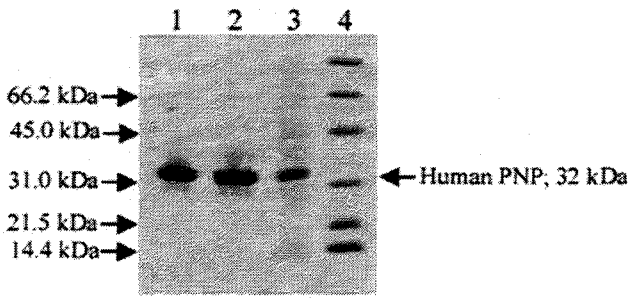

Fig. 3. SDS-PAGE analysis of pooled fractions from the various purification protocol steps. Lane 1, S-200 gel filtration; lane 2, Q-Sepharose Fast Flow ion exchange; lane 3, crude extract; lane 4, MW markers.

However, PNP is estimated to make up only 0.04% of the total protein in human erythrocytes and purification protocol involves a number of steps resulting in only 1.2 mg of homogeneous human PNP from 130 ml of freshly drawn blood [24]. Recombinant human PNP expressed in *E. coli* cells has been shown to represent approximately 5% of the soluble protein cell homogenates [20]. However, the purification protocol using a dye-matrix resin and isoelectrofocusing chromatography yielded about 2.6 mg of purified recombinant human PNP from 1.0 g of cells [20]. Therefore, to the best of our knowledge, the straightforward two-step purification protocol (ion exchange and gel filtration) associated with high expression of the target protein (42%), which results in a yield of approximately 12 mg of soluble and functional protein from 1.0 g of cells, represents a significant improvement on previous methods of expression and separation of recombinant human PNP.

The subunit molecular mass of active human PNP was determined to be 31,966 Da by electrospray ionization mass spectrometry (ESI-MS), consistent with the post-translational removal of the N-terminal methionine residue from the full length gene product (predicted mass: 32,097 Da). The ESI-MS result revealed no peak at the expected mass for *E. coli* PNP (25,950 Da), thus, providing evidence for both the identity and purity of the recombinant human protein. The first nine N-terminal amino acid residues of the recombinant protein were identified as ENGYTYEDY by the Edman degradation method. This result unambiguously identifies the recombinant protein as human PNP and confirms removal of the N-terminal methionine residue from it. A common type of co-/post-translational modification of proteins synthesized in prokaryotic cells is modification at their N termini. Methionine aminopeptidase catalyzed cleavage of initiator methionine is usually directed by the penultimate amino acid residues with the smallest side chain radii of gyration (glycine, alanine, serine, threonine, proline, valine, and cysteine) [27]. Interestingly, the *E. coli* expressed recombinant human PNP enzyme seems not to conform to this rule, since the

Table 2
Purification of human purine nucleoside phosphorylase from *E. coli* BL21(DE3) [pET23a(+)::*pnp*] cells

Purification step	Protein (mg)	Units (U)	Sp act[a] ($U mg^{-1}$)	Purification fold	Yield (%)
Crude extract	382.95	9569.92	25	1.0	100
Ion exchange	66.42	4994.12	75	3.0	52
Gel filtration	48.10	3851.84	80	3.2	41

[a] $U ml^{-1}/mg ml^{-1}$.

N-terminal methionine was removed, despite the penultimate amino acid residue being a charged residue (glutamate).

As previously pointed out, there are a number of potential applications for human PNP. From the viewpoint of biotechnological tools development, a bacterial enzyme has been used to follow P_i release kinetics [9] and human PNP has been studied for its application in purine nucleoside analog synthesis [25,26]. The commercially available "bacterial" protein used in continuous spectrophotometric assay for P_i detection has been shown to be about one-third PNP by weight [10] and to contain a large content of albumin [14], which may require further purification for its use in coupled assays. From the viewpoint of drug development, inappropriate activation of T-cells has been proposed or documented in several clinically relevant human conditions, such as transplant tissue rejection, psoriasis, rheumatoid arthritis, T-cell lymphomas, and lupus. Since genetic deficiency of human PNP causes T-cell deficiency as the major physiological defect, specific PNP inhibitors may provide useful agents for these disorders. Accordingly, a transition-state analog (Immucillin-H) that inhibits PNP enzyme activity has been shown to inhibit the growth of malignant T-cell leukemia cell lines with the induction of apoptosis [28].

The real-time BIA from Pharmacia Biosensor AB (BIACORE), which is a label-free technology for monitoring biomolecular interactions as they occur, was chosen for high-throughput drug screening studies. The detection principle of BIACORE equipment relies on surface plasmon resonance (SPR), an optical phenomenon that arises when light illuminates thin conducting films under specific concitions. Direct immobilization of protein ligands is possible through linkages between the *N*-hydroxy-succinimide (NHS) ester groups on a hydrophilic dextran matrix and amine groups on proteins. In protein molecules, NHS ester cross-linking reagents couple principally with the α-amines at the N-terminals and the ε-amines of lysine side chains [29]. Since human PNP protein has 12 lysine residues in its primary sequence, it is likely that immobilization of the recombinant protein will not present difficulties. The work presented here represents a crucial step in our efforts towards both using immobilized human PNP enzyme as a target for drug development in high-throughput drug screening and testing its suitability as a tool for coupled enzymatic assay. Moreover, since the deposited atomic coordinates of human PNP (PDB access codes: 1ULA and 1ULB) have been withdrawn due to low resolution, the work presented here also provides protein in quantities necessary for crystallographic studies. Indeed, we have recently deposited the atomic coordinates of the crystal structure of the recombinant human PNP protein solved at 2.3 Å resolution (PDB access code: 1M73).

Acknowledgments

Financial support for this work was provided by Millenium Initiative Program MCT-CNPq, Ministry of Health—Secretary of Health Policy (Brazil) to D.S.S. and L.A.B. D.S.S. and L.A.B. also acknowledge grants awarded by CNPq and FINEP. We thank Marcelo Brígido for his generous gift of human cDNA library, Denise Machado for assistance in human liver cDNA library expansion, and Deise Potrich for nucleotide sequence analysis.

References

[1] R.E. Parks Jr., R.P. Agarwal, in: P.D. Boyer (Ed.), The Enzymes, Academic Press, New York, 1972, pp. 483–514.
[2] V.L. Schramm, Enzymatic transition states and transition state analog design, Annu. Rev. Biochem. 67 (1998) 693–720.
[3] J.D. Stoeckler, C. Cambor, R.E. Parks Jr., Human erythrocytic purine nucleoside phosphorylase: reaction with sugar-modified nucleosides substrates, Biochemistry 19 (1980) 102–107.
[4] D.J.T. Porter, Purine nucleoside phosphorylase. Kinetic mechanism of the enzyme from calf spleen, J. Biol. Chem. 267 (1992) 7342–7351.
[5] A.S. Lewis, B.A. Lowy, Human erythrocytes purine nucleoside phosphorylase: molecular weight and physical properties, J. Biol. Chem. 254 (1979) 9927–9932.
[6] W. Stoop, B.J.M. Zegers, G.F.M. Hendrickx, L.H.S. van Heukelom, G.E.J. Staal, P.K. de Bree, S.K. Wadman, R.E. Ballieux, Purine nucleoside phosphorylase deficiency associated with selective cellular immunodeficiency, N. Engl. J. Med. 296 (1977) 651–655.
[7] B.S. Mitchell, E. Meijias, P.E. Daddona, W.N. Kelley, Purinogenic immunodeficiency diseases: selective toxicity of deoxyribonucleosides for T-cells, Proc. Natl. Acad. Sci. USA 75 (1978) 5011–5014.
[8] J.D. Stoeckler, in: R.I. Glazer (Ed.), Developments in Cancer Chemotherapy, CRC Press, Boca Raton, FL, 1984, pp. 35–60.
[9] L.L. Bennett Jr., P.W. Allan, P.E. Noker, L.M. Rose, S. Niwas, J.A. Montgomery, M.D. Erion, Purine nucleoside phosphorylase

inhibitors: biochemical and pharmacological studies with 9-benzyl-9-deazaguanine and related compounds, J. Pharm. Exp. Ther. 266 (1993) 707–714.

[10] M.R. Webb, A continuous spectrofotometric assay for inorganic phosphate and for measuring phosphate release kinetics in biological systems, Proc. Natl. Acad. Sci. USA 89 (1992) 4884–4887.

[11] M. Brune, J. Hunter, J.E.T. Corrie, M.R. Webb, Direct, real-time measurements of rapid inorganic phosphate release using a novel fluorescent probe and its application to actinomyosin subfragment 1 ATPase, Biochemistry 33 (1994) 8262–8271.

[12] Z.X. Wang, Q. Cheng, S.D. Killilea, A continuous spectrophotometric assay for phosphorylase kinase, Anal. Biochem. 230 (1995) 55–61.

[13] Q. Cheng, Z.X. Wang, S.D. Killilea, A continuous spectrophotometric assay for protein phosphatases, Anal. Biochem. 226 (1995) 68–73.

[14] A.E. Nixon, J.L. Hunter, G. Bonifacio, J.F. Eccleston, M.R. Webb, Purine nucleoside phosphorylase: its use in a spectroscopic assay for inorganic phosphate and for removing inorganic phosphate with aid of phosphodeoxyribomutase, Anal. Biochem. 265 (1998) 299–307.

[15] S.R. Williams, J.M. Goddard, D.W. Martin Jr., Human purine nucleoside phosphorylase cDNA sequence and genomic clone characterization, Nucleic Acids Res. 12 (1984) 5779–5787.

[16] U.K. Laemmli, Cleavage of structural proteins during the assembly of the head of bacteriophage T4, Nature 227 (1970) 680–685.

[17] M.M. Bradford, R.A. McRorie, W.L. Williams, A rapid and sensitive method for the quantitation of microgram quantities of protein utilizing the principle of protein–dye binding, Anal. Biochem. 72 (1976) 248–254.

[18] H. Chassaigne, R. Lobinski, Characterization of horse kidney metallothionein isoforms by electrospray MS and reversed-phase HPLC-electrospray MS, Analyst. 123 (1998) 2125–2130.

[19] J.M. Goddard, D. Caput, S. Williams, D.W. Martin, Cloning of human purine nucleoside phosphorylase cDNA sequences by complementation in *Escherichia coli*, Proc. Natl. Acad. Sci. USA 80 (1983) 4281–4285.

[20] M.D. Erion, K. Takabayashi, H.B. Smith, J. Kessi, S. Wagner, S. Hönger, S. Shames, S. Ealick, Purine nucleoside phosphorylase. 1. Structure–function studies, Biochemistry 36 (1997) 11725–11734.

[21] K.C. Kelley, K.J. Huestis, D.A. Austen, C.T. Sanderson, M.A. Donoghue, S.K. Stickel, E.S. Kawasaki, M.S. Osburne, Regulation of *sCD4-183* gene expression from phage-T7-based vectors in *Escherichia coli*, Gene 156 (1995) 33–36.

[22] J.S. Oliveira, C.A. Pinto, L.A. Basso, D.S. Santos, Cloning and overexpression in soluble form of functional shikimate kinase and 5-enolpyruvylshikimate 3-phosphate synthase enzymes from *Mycobacterium tuberculosis*, Protein Expr. Purif. 22 (2001) 430–435.

[23] T.H. Grossman, E.S. Kawazaki, S.R. Punreddy, M.S. Osburne, Spontaneous cAMP-dependent derepression of gene expression in stationary phase plays a role in recombinant expression instability, Gene 209 (1998) 95–103.

[24] V. Zannis, D. Doyle, D.W Martin Jr., Purification and characterization of human erythrocyte purine nucleoside phosphorylase and its subunits, J. Biol. Chem. 253 (1978) 504–510.

[25] J.D. Stoeckler, F. Poirot, R.M. Smith, R.E. Parks Jr., S.E. Ealick, K. Takabayashi, M.D. Erion, Purine nucleoside phosphorylase. 3. Reversal of purine base specificity by site-directed mutagenesis, Biochemistry 36 (1997) 11749–11756.

[26] M.D. Erion, J.D. Stoeckler, W.C. Guida, R.L. Walter, S.E. Ealick, Purine nucleoside phosphorylase. 2. Catalytic mechanism, Biochemistry 36 (1997) 11735–11748.

[27] W.T. Lowther, B.W. Matthews, Structure and function of the methionine aminopeptidases, Biochim. Biophys. Acta 1477 (2000) 157–167.

[28] G. Kicska, L. Long, H. Hörig, G. Fairchild, P.C. Tyler, R.H. Furneaux, V.L. Schramm, H.L. Kaufman, Immucilli H, a powerful transition-state analog inhibitor of purine nucleoside phosphorylase, selectively inhibits human T lymphocytes, Proc. Natl. Acad. Sci. USA 98 (2001) 4593–4598.

[29] G.T. Hermanson, in: Bioconjugate Techniques, Academic Press, San Diego, 1996, pp. 137–168.